REPORT DOCUMENTATION PAGE

Form Approved
OMB No. 0704-0188

1. REPORT DATE *(DD-MM-YYYY)*	2. REPORT TYPE	3. DATES COVERED *(From - To)*
03-17-2008	FINAL REPORT	From 1Sept06 to 30Jun07

4. TITLE AND SUBTITLE
NOVEL PIXILATED POLARIMETER AND ASSOCIATED NANOIMPRINTING TECHIQUES, TO ADDRESS ADVANCED IMAGING APPLICATIONS

5a. CONTRACT NUMBER
FA9550-07-C-0012

5b. GRANT NUMBER

5c. PROGRAM ELEMENT NUMBER

6. AUTHOR(S)
Wang, Jian, J., NanoOpto Corporation
Guo, Jay, L., University of Michigan

5d. PROJECT NUMBER

5e. TASK NUMBER

5f. WORK UNIT NUMBER

7. PERFORMING ORGANIZATION NAME(S) AND ADDRESS(ES)
NanoOpto Corporation 1600 Cottontail Lane Somerset, NJ 08873

8. PERFORMING ORGANIZATION REPORT NUMBER

9. SPONSORING/MONITORING AGENCY NAME(S) AND ADDRESS(ES)
Pomrenke, Gernot S., AFOSR/NE
801 N. Randolph Street, Rm. 732
Arlington, VA 22203
703-696-8426

10. SPONSOR/MONITOR'S ACRONYM(S)

11. SPONSOR/MONITOR'S REPORT NUMBER(S)

12. DISTRIBUTION/AVAILABILITY STATEMENT
DISTRIBUTION STATEMENT A: UNLIMITED

AFRL-SR-AR-TR-08-0169

13. SUPPLEMENTARY NOTES

14. ABSTRACT
The final objective of this contract is to improve nano-optical sub-components and then further to demonstrate a monolithically integrated nano-optical pixilated-array polarimeter. In parallel, part of the goal of this project is also to develop a low-cost web-to-web nanoimprint system/method/process for more efficiently making low-cost nano-structured optical devices directly onto plastic sheets.

In the final report, we will report and summarize all the results and progresses which we have made during the whole phase-I program. We have made tremendous progress during this program. The results outperform our original expectation.

15. SUBJECT TERMS
Nano-optical component, nanoimprint lithography, roller nanoimprint, nano-wire-grid polarizer, nano-optical wave plate

16. SECURITY CLASSIFICATION OF:			17. LIMITATION OF ABSTRACT	18. NUMBER OF PAGES	19a. NAME OF RESPONSIBLE PERSON
a. REPORT	b. ABSTRACT	c. THIS PAGE			Jian Jim Wang
U	U	U	UU	39	19b. TELEPHONE NUMBER *(Include area code)* 732-735-5620

Project: **NOVEL PIXILATED POLARIMETER AND ASSOCIATED NANOIMPRINTING TECHIQUES, TO ADDRESS ADVANCED IMAGING APPLICATIONS**

Principal Investigator: **Dr. Jian Jim Wang**
Chief Technical Officer
NanoOpto Corporation
1600 Cottontail Lane
Somerset, NJ 08873
Email: jwang@nanonuvo.com; Phone: (732) 735-5620

Co-Principal Investigator: **Prof. L. Jay Guo**
Department of Electrical Engineering and Computer Science
The University of Michigan
1301 Beal Ave., Ann Arbor, MI 48109
Email: guo@umich.edu; Phone: (734) 647-7718

Subject: **Final Report – Contract FA9550-07-C-0012**

Date: **15 June 2007**

Report Contents:

1. Executive Summary

This is the final report for the contract **FA9550-07-C-0012.** The goal of this contract is to improve nano-optical sub-components and then further to demonstrate a monolithically integrated nano-optical pixilated-array polarimeter. In parallel, part of the goal of this project is also to develop a low-cost web-to-web nanoimprint system/method/process for more efficiently making low-cost nano-structured optical devices directly onto plastic sheets.

In the final report, we will report and summarize all the results and progresses which we have made during the whole phase-I program.

We have made tremendous progress during this program. The results outperform our original expectation.

2. The novel pixilated polarimeter for advanced imaging applications

A great deal of valuable information can be obtained about an entity through novel imaging methods. Recently, multi-spectral and hyperspectral imaging systems have enabled increasing amounts of information to be gained by imaging scenes, usually from the air, such as regions of vegetation or mineral deposits over a number of wavelength bands from the UV through MWIR spectral regions. Many defense and aerospace applications also use these imaging techniques to gain considerably more information than is available simply by imaging over a specific spectral region.

In the same way, even more characteristics about a scene or an entity can be discerned through imaging polarimetry, or imaging by polarization state. Any smooth object which reflects un-polarized light may not reveal crucial information about the object, thus polarization techniques will help enable the accumulation of such information. For example, biological tissues such as collagen, retinal tissue, keratin, and myelin are all polarization sensitive. Imaging by polarimetry is therefore a valuable medical diagnostic tool. In fact, any imaging system or industry which makes use of imaging can be enhanced by including polarization information, due to the increased contrast and/or polarization-sensitive characteristics which the imaged entity or scene might possess. Other examples are ice detection under conditions of poor visibility, industrial applications such as machining, agriculture, geological/vegetation/wildlife surveying, microscopy, medical imaging equipment, gas detection, minefield detection, detection of hidden objects in general, details in the atmosphere, and security. Military applications may include target acquisition and identification, as artificial objects may be revealed with respect to natural background and countermeasures due to the increased contrast.

In order to further advance existing imaging technology, and to address these future imaging requirements, NanoOpto is developing a pixilated polarimeter, designed to be used in conjunction with imaging sensors of all types, including focal plane arrays. Phase 1 would culminate in the demonstration of this device. If invited to participate in Phase 2, the device would be further developed to be integrated with the image sensor, perhaps along with a bandpass filter if required.

Scientists from the Raytheon Corporation have been shown the concept proposed here, and have expressed strong interest in this development, due to the many enhancements that such a device would provide to evolving imaging systems. Raytheon has provided a letter of endorsement to the STTR POC, in support of this development.

Parallel to NanoOpto's effort, the Guo group at the University of Michigan (UM) is working on an alternative approach to develop a roll-to-roll continuous imprinting technology to fabricate such polarizer elements on flexible web. This is a very novel approach, which not only complements the NanoOpto's effort, but will also lead to major breakthroughs in high-speed fabrication of photonic nanostructures that can find applications in polarimeters, LCD displays and OLED displays, to name an important few. To produce a pixilated polarimeter, the UM's approach is to laminate a thin sheet containing the pixilated polarizer elements to an existing CCD or CMOS imaging device. Because the NanoOpto Corporation addresses the projection display industry with its polarization technology, and because of the ease of manufacturing that this nanoimprinting technology would provide to mass-producing the pixilated polarimeter, there is great interest within the company in this new technology that will be developed at the University of Michigan.

In this first phase of development, NanoOpto is to develop a pixilated polarimeter, which is operational over the spectral region 300-2000nm (although we additionally have the capability of depositing a similar structure from 1-5μm on a silicon substrate). The structure is designed to be used in conjunction with a focal plane array as part of the optical design in an imaging system. Each pixel will have a distinct polarization state, such that the resulting array allows the Stokes vectors (which are used to characterize the polarization states) to be determined. Two of the polarization states will be repeated and integrated with a quarter waveplate in an additional two pixels. The pixel size depends on the application but the suggested size is 10 μm x 10 μm in Phase 1.

The pixel characteristics are planned as follows:

1. Each of four of the pixels will have one of four linear polarization orientations - 0°, 45°, 90°, and 135°. There will be two additional pixels, with 45° and 135° orientations, and these will be integrated with a quarter waveplate, as shown, providing the two states of circular polarization, as shown in the following schematic. The arrangement of angles in the array can be arranged as required, as long as the same array is repeated in each pixel across the entire device. This arrangement of six pixels will be regularly repeated throughout the array.

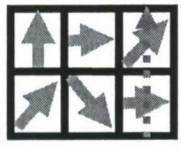

2. The pixel size will be 10μm x 10μm, unless otherwise required. The boundaries between pixels will be 0.2 μm. NanoOpto is capable of defining pixel sizes as small as 3 μm. However, the smaller the pixel, the greater will be the effects of the boundaries. This pixel size will be compatible with silicon detectors. The pixel size can be made larger, e.g. ~25μm x 25μm, for longer wavelength detectors.

3. The size of the entire pixilated polarimeter will be 1024 x 768 pixels, or 10.24 x 7.68mm, for the final application.

4. The pixel clear aperture will be determined based on the given pixel size and boundary effects.

5. The wavelength range will be from 300-2000nm, spanning through the UV/NIR spectral regions. This can be specified according to the requirement/application.

6. The substrate material will be fused silica glass, for the wavelength range chosen. The thickness is 0.5mm. For integration with an image sensor, the device can be made thinner, typically 0.1 – 0.2mm by back side polishing and thinning.

Polarization information from the six pixels which are engaged in imaging the associated part of the scene or entity will be cascaded from pixel to pixel, and gathered and interpreted according to the algorithms of the imaging system, as in the operation of a CCD device.

Figure 1 shows a schematic of a cross-section of part of the structure, with adjacent circular and linear polarizer pixels, to illustrate the structure and fabrication steps for the device.

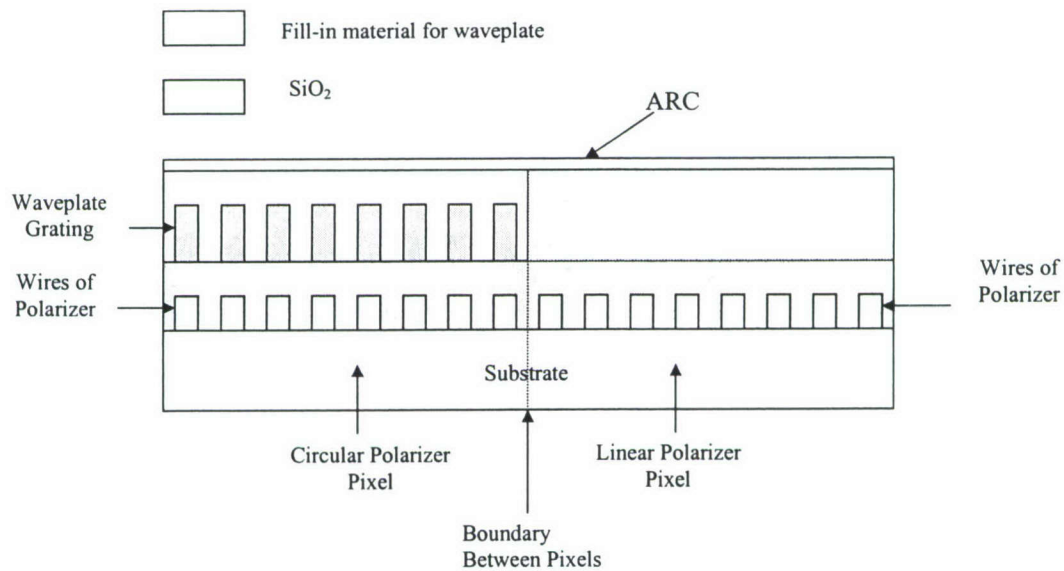

Figure 1 Schematic of Cross-section of adjacent circular and linear polarizer pixels

Parallel to NanoOpto's efforts in this first phase of development, UM team is developing the materials, processing techniques and simple prototype roller imprinter for a proof-of-concept demonstration. They also design and simulate the polarization properties based on a new wire-grid polarizer configuration that can be fabricated in a continuous web-

processing environment. Since this is an entirely new development that is based on a recent invention disclosure filed at the University of Michigan, the Phase 1 project focus on the feasibility study of continuous processing of polarizing elements, but not on pixilated polarizers. The UM team make this choice primarily because of the limited time and funding during Phase 1. But once the concept is proved in the experiment, we anticipate no significant difficulty in extending the technique to make pixilated polarizer elements of the type which will be demonstrated during NanoOpto's efforts in Phase 1.

For this novel pixilated polarimeter, all the sub-components, such as polarizers and waveplates, are designed and fabricated using the nano-optical concepts and nanofabrication methods. The nanotechnology approach is seen as the only feasible approach to lead to such monolithically integrated pixilated polarimeter chips.

3. Report on various nano-optical sub-components for advanced imaging applications

In order to realize the novel monolithically integrated nano-optical polarimeter, we need to realize all the sub-components first. The sub-components include nanowire-grid polarizer which covers the visible and IR bands from 450 nm to 2 microns, nanowire-grid polarizer which covers from deep ultraviolet 250 nm to IR bands, nanowire-grid polarizer directly imprinted onto a plastic PET substrates, and nano-optical waveplate (i.e., retarder).

3.1 Nanowire-grid visible polarizer (operating from 400 nm to > 2 μm)

The wire-gird polarizer consists of fine grid of parallel metal wires with spacing and width less than wavelength of light. Inorganic wire-grid visible polarizers are crucial for applications such as front and back liquid-crystal display (LCD) projection displays and televisions due to their durability under exposure to high UV flux and high temperature environment. Current commercially available such polarizers have a low performance combination for contrast and transmittance.

The key parameters that determines the performance (e.g., extinction ratio) of a wire grid polarizer is period (i.e., the center-to-center spacing), linewidth and depth of the grid elements. It was realized that lithography is needed to make good quality wire-grid polarizers. Since metal wire-grids suffer from internal metal absorption and scattering loss caused by non-perfect structure, it is very difficult to make commercial quality wire-grid polarizers. In order to do so, both process related issues (i.e. lithography) and design related issues need to be considered and optimized. Through the past few years, we continue developing a new type of metal wire-grid polarizers (polarizing beam splitters), so called nanowire-grid polarizer (polarizing beam splitter (PBS)), for a broadband (< 400 nm to > 2000 nm) applications. The fabrication of the nanowire is based on wafer-level nanoimprint lithography, which produces large size (e.g., 4" in-diameter) polarizers.

We have achieved both high contrast and high transmittance with the nanowire-grid polarizers. Aluminum nanowire-grid polarizers with 30-nm wide linewidth and 200-nm depth were fabricated by UV-nanoimprint lithography.

Rigorous coupled-wave analysis was used to simulate the nanowire-grid polarizers. In-house compiled software codes implemented the rigorous coupled wave analysis and modal methods.

For a general wire-grid polarizer, three parameters are used to characterize a polarizer's performance: transmission contrast ratio (CR), total energy efficiency (P), and TM transmittance (T). Transmittance (T) is the power transmission coefficient for TM (electric-field vector perpendicular to the wire) polarized light. CR is defined as T/T_{TE}, in which T_{TE} is the power transmission coefficient for TE (electric-field vector parallel to the wire) polarized light. P is defined as $T + R_{TM}$ or $1 - loss_{TM}$ where R_{TM} is the power reflection coefficient for TM polarized light. P is a key parameter for characterizing the wire-grid polarizer, since P is always less than 1 (or 100%) for a wire-grid polarizer because of the existence of internal energy loss (e.g., metal absorption, light-scattering loss). One important goal for a wire-grid polarizer is to achieve as high as possible P while maintaining enough CR. Once the period of the wire grid is determined, there is always an inherent trade-off between achieving high P and high CR because achieving higher CR requires more metal volume which leads to more absorption and thus lower P. In general, a shorter period is preferred which extends the operation wavelength of the polarizer into shorter wavelength. If the period is long compared to the wavelength, the wire grid functions as a diffraction grating rather than a polarizer. It diffracts both polarizations according to well-known principles. When the period is much shorter than the wavelength, the wire grid functions as a polarizer. Due to technology limitation, it is difficult to achieve small period. In this work, a period of ~ 146 nm is used.

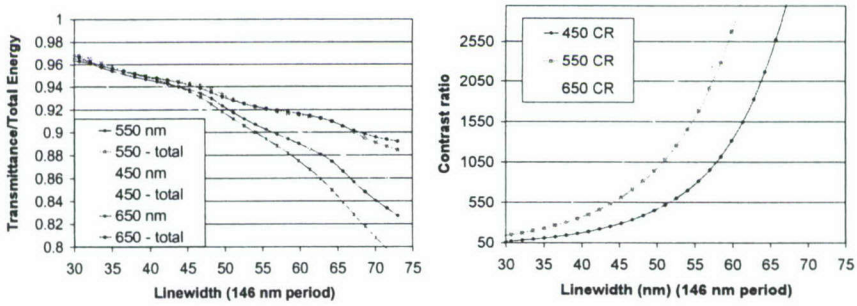

Fig. 2 Simulation to show linewidth of Al wire is the most important parameter which determines the transmittance efficiency. TM transmittance and TM total energy (top), as well as the contrast ration (bottom) at three different wavelengths, i.e., 450nm, 550nm and 650nm, respectively, are calculated as the function of the linewidth. The Al wires have a rectangular shape with a period of 146 nm and a depth of 150 nm.

In Fig. 2, simulation results from a rectangular-shaped aluminum wire-grid polarizer are shown. A fixed depth of 150 nm for the aluminum nanowire-grid was used. Transmittance for TM, total energy for TM and contrast ratio were calculated as function of linewidth at three discrete wavelengths of 450 nm, 550 nm and 650 nm, respectively. The period of the nanowire-grid is 146 nm. It is seen that both the TM total energy and transmittance are very sensitive to the linewidth of the nanowire-grid. Increasing linewidth leads to a fast drop on the total energy and therefore transmittance. In contrast, increasing linewidth leads to a fast increase on the contrast ratio. The trade-off between the transmittance and the contrast is clearly reflected. In the modeling, since the simulation assumes aluminum nanowire-grid with perfect linewidth, shape, smoothness, surface condition and material property, the experimental values of the transmittance and contrast, particularly the contrast ratio, are lower than the simulated data. It is clearly shown that linewidth of Al wire is the most important parameter which determines the transmittance efficiency.

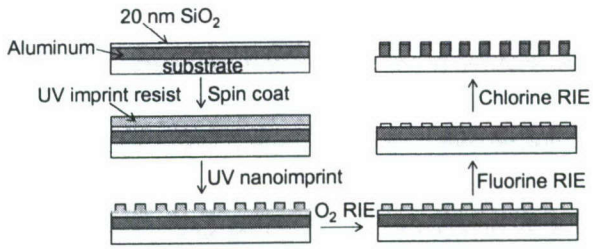

Fig. 3 A schematic process flow to achieve very narrow linewidth Al nano-wire grids.

Fabrication process is crucial to realize a wire-grid polarizer with optimal optical performance. The process flow for fabrication of the nanowire-grid polarizer is schematically shown in Fig. 3. We start with a 4" in-diameter BK7 glass wafer which has a thickness of ~ 0.5 mm. The bottom anti-reflective coatings can be deposited either prior to or after fully completing the front side nanowire-grid structures. The front surface was coated with a layer of high-purity aluminum by high-vacuum e-beam deposition. A thin layer (~ 20 nm) of SiO_2 was then coated onto the aluminum layer by e-beam deposition, which functions as a hard mask for later on aluminum etching. A thin layer of home-prepared UV-curable nanoimprint resist (OP133) with a thickness of ~ 150 nm was then spun coated on. The UV-nanoimprint process was then used to form the resist pattern. A 4" in-diameter fused silica grating mold with a period of 146 nm was used in the UV-nanoimprint process. We used newly developed immersion interference lithography to make the mold with 146 nm period. The immersion interference lithography was used to fabricate 4" in-diameter nanoimprint molds on fused silica substrates. The whole UV-nanoimprint process took only about few minutes. The patterned resist has a period of 146 nm with a resist line width of about 50 nm and a height of about 100 nm. There was a continuous and uniform resist residual layer with a thickness of about 100 nm underneath the resist lines. In order to expose the underneath SiO_2 layer between the patterned resist lines, a blank oxygen reactive ion etching (RIE) (3 mtorr, 50 W, 4 sccm) with varied etching depths was conducted in order to achieve different resist linewidths prior to etching of the SiO_2 hard mask. After that, an RIE process with CHF_3 (5 mtorr, 100 W, 10 sccm) was used to etch 20 nm SiO_2 with the polymer resist line as masks. Finally, a chlorine-based RIE process (60 sccm BCl_3 and 50 sccm Cl_2 at 5 mtorr) was used to etch aluminum layer into aluminum nanowire-grid by using the patterned SiO_2 as etching hard mask. The final linewidth of the aluminum wires is determined by the linewidth of the SiO_2 hard mask, which can be controlled by the linewidth of the mold and the blank oxygen RIE etch depth.

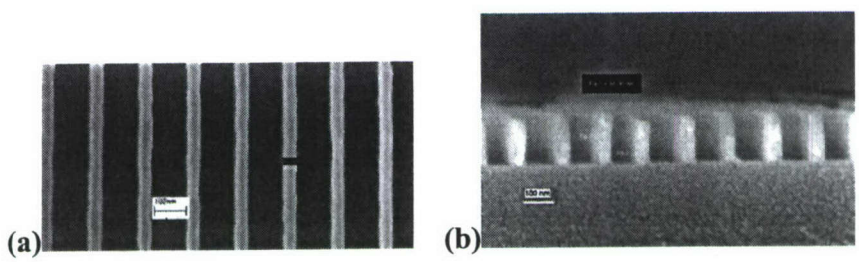

Fig. 4 A top SEM view photograph of an aluminum nanowire-grid polarizer with ~ 40 nm linewidth (a), and a cross-sectional SEM photograph of an aluminum nanowire-grid polarizer with a linewidth of 33 nm (b).

Since both high contrast and high transmittance are preferred for all the applications, in this work, we achieved ultra-high contrast along with high transmittance through reducing linewidth of the nanowire-grid polarizer down to 40 nm to 30 nm. Fig. 4(a) shows a top-view SEM photograph of an aluminum nanowire polarizer with a linewidth of ~ 40 nm and a depth of ~ 200 nm. Fig. 4(b) shows cross-sectional SEM photography of an aluminum nanowire with a linewidth of ~ 33 nm and a depth of ~ 200 nm.

For the measurement, we used a spectrometer measurement system (Axometrics) based on a lamp covering 400 nm to 800 nm. All the measurements as well as the simulation results in this work were performed at close to normal incidence. Fig. 5 shows the optical performance of both transmittance and contrast for a polarizer with 33 nm linewidth and 200 nm depth. A record high transmittance of up to 95% was achieved. However, the contrast is low, i.e., only 100 – 300: 1 in the visible range. To achieve a high contrast, we fabricated the 30 nm wide aluminum nanowire structures on the both sides of the glass wafers. Fig. 6 shows the optical performance of a two-side polarizer. It is seen that an extremely high contrast up to 10,000:1 was achieved along with good transmittance of 83% to 87%. Compared with all existing thin-film type polarizers and, in particular, the wire-grid visible polarizer, the approach we present here clearly offer a better contrast and transmittance.

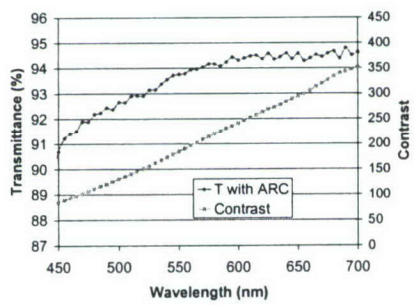

(4)

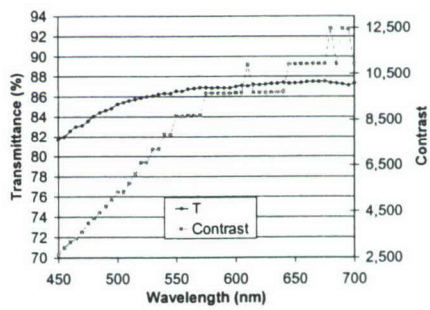

(5)

Fig. 5 Optical performance (transmittance and contrast) of an aluminum nanowire-grid polarizer with 33 nm linewidth, 145 nm period and 200 nm depth. Fig. 6 Optical performance (transmittance and contrast) of a double-side aluminum nanowire-grid polarizer with 33 nm linewidth, 145 nm period and 200 nm depth.

3.2 Nanowire-grid polarizer (operating from deep-ultraviolet 250 nm to > 2μm)

The key parameters that determines the performance (e.g., extinction ratio) of a WGP is period (i.e., the center-to-center spacing), linewidth and depth of the grid elements. It is shown above that, once the pitch of the WGP is fixed, transmittance is very sensitive to the linewidth of the nanowire-grid. Linewidth of the metal wire is the most important parameter which determines the transmittance efficiency. The pitch of the WGP is the other key parameter that determines the operating bandwidth and performance, i.e., extinction ratio. In general, smaller pitches enable the WGP to work effectively at shorter wavelengths. Furthermore, within the operating bandwidth, the smaller the pitch is, the better the extinction ratio across the band is. As a general rule of thumb, the shortest operating wavelength of a WGP can work efficiently as a polarizer is about 3 times of the pitch. Current commercially available WGP has a pitch of about 150 nm due to nanofabrication challenges, which limits it to an effective operating wavelength down to ~ 450 nm, also, a contrast ratio of about 500: 1 to 2000: 1 in the visible wavelength band. Although there

were research work on UV polarizer with wire-grids, the achieved performance is far from any practical/commercial applications.

In this work, we successfully fabricated large-area aluminum nano-wire grids with 40-nm line/78 nm space and 118 nm pitch, which perform as a highly efficient optical polarizer for deep ultraviolet wavelength down to ~ 250 nm. In addition, an extremely high contrast from 10,000:1 to 50,000:1 was achieved across the whole visible and near-infrared wavelength range, along with good transmittance (85% to 90%).

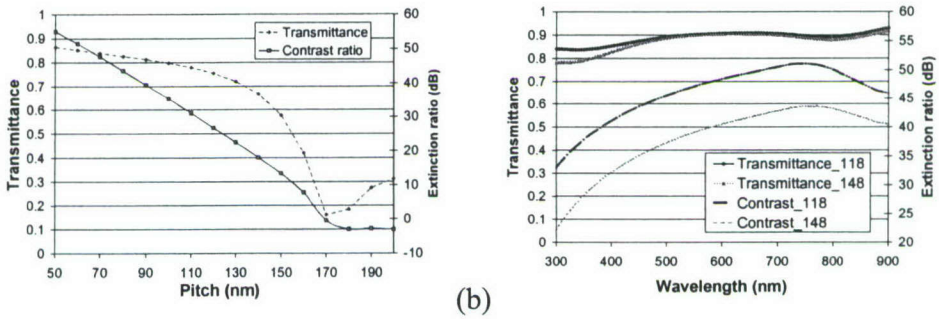

Fig. 7 Simulation results from rectangular-shaped aluminum WGPs are shown. Fig. 7(a) shows the simulation results of WGP's transmittance and extinction ratio (in dB), at a DUV wavelength of 266 nm, as function of pitch from 200 nm to 50 nm. Fig. 7(b) shows simulation results for both transmittance and extinction ratio (in dB) as function of wavelength, from 300 nm to 900 nm, with two WGPs, one has a pitch of 118 nm and the other one has 148 nm.

In Fig. 7, simulation results from rectangular-shaped aluminum WGPs are shown. Fig. 7(a) shows the simulation results of WGP's transmittance and extinction ratio in dB, at a DUV wavelength of 266 nm, as function of pitch from 200 nm to 50 nm. A fixed depth of 200 nm and a fixed duty cycle (i.e., width of the wire divided by the pitch) of 34% for the aluminum nanowire-grid were used. It shows that a shorter pitch than 130 nm is required to achieve good polarizing property, i.e., extinction ratio and transmittance, at the DUV wavelength of 266 nm. Also, shorter periods give better performance. Fig. 7(b) shows simulation results for both transmittance and extinction ratio (in dB) as function of wavelength, from 300 nm to 900 nm, for two WGPs. Both of the WGPs have a depth of 200 nm, but one has a pitch of 118 nm and one has 148 nm. The same duty cycle of 34% was used. It is clear that polarizer performance, in particular the contrast, is significantly improved across the whole band with a shorter pitch.

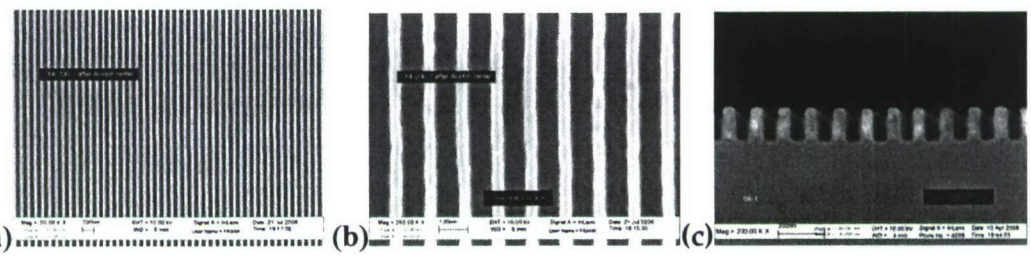

Fig. 8(a) A top SEM view photograph of an aluminum nanowire-grid polarizer with ~ 40 nm linewidth and ~ 59 nm half-pitch. Fig. 8(b) shows a zoom-in view. Fig. 8(c) shows a cross-sectional SEM view.

The choice of nanofabrication process is crucial to realize such WGPs with short pitch and narrow linewidth. Large area small-pitch structures, such as 40 nm linewidth and 58 nm half-pitch, are very difficult to fabricate by all of the existing technologies, including DUV photolithography, E-beam lithography and X-ray lithography. We used deep-UV interference lithography to make a 118-nm period structure on a 100-mm-diameter wafer. Interference lithography, or so called holographic lithography, is an important technique to generate large area periodic or quasi-periodic structures. For a two-beam setup, the period (Λ) of the interference pattern is described by the following formula: $\Lambda = \lambda/(2\sin(\theta/2))$, where, λ is the wavelength of the laser source, and θ is the angle between the two beams. The smallest period can only approach $\lambda/2$. A continuous-wave single-frequency deep-ultraviolet laser of 266 nm, frequency-doubled from a solid state Nd-YAG 532 nm laser, was used. A two-beam interference setup with a 110° angle between the two beams was used. In air, the system produced a uniform 100-mm-diameter grating with a ~ 148-nm period. In order to reach a shorter period, a full-wafer immersion technique was used. A triangular liquid cell was inserted into the two-beam interference lithography setup where a photoresist-coated wafer was immersed completely into the liquid cell. By this technique, with the same laser source, the period of the interference pattern was reduced by a factor of n, where n is the refractive index of the liquid used. For water, n is around 1.35 at 266 nm. Another key advantage of such immersion interference lithography technique is that the same resist system as used in air can be used since the frequency of the laser is not changed.

For making the nanowire grid polarizer, we started with a 100-mm-diameter fused silica wafer coated on one side with a 200-nm thick aluminum film by high vacuum e-beam evaporation. The bottom anti-reflective coatings can be deposited either prior to or after fully completing the front side nanowire-grid structures. A thin layer (~ 20 nm) of SiO_2 was then coated onto the aluminum layer by e-beam deposition, which functions as a hard mask for later on aluminum etching. Then a thin layer (~180 nm) of S-1805 photoresist was spin-coated. The immersion interference lithography was used to pattern the photoresist with a 118-nm period according to the above description. After exposure and photoresist development, an RIE process with CHF_3 (5 mtorr, 100 W, 10 sccm) was used to etch 20 nm SiO_2 with the polymer resist line as masks. Finally, a chlorine-based reactive ion etching (RIE) with 60 sccm BCl_3 and 50 sccm Cl_2 at 5 mtorr was then used to etch aluminum into aluminum nano-gratings by using the patterned SiO_2 as etching hard mask. The etching time for the 200-nm-thick aluminum was about 25 seconds. The final linewidth of the aluminum wires is determined by the linewidth of the SiO_2 hard mask, which can be controlled by the linewidth of the photoresist and the blank oxygen RIE etch depth.

Since both high contrast and high transmittance are preferred for all the applications, we achieve ultra-high contrast through reducing the period of the aluminum wire-grid and high transmittance through reducing linewidth of the nanowire down to 40 nm. Fig. 8(a) shows a top view SEM photograph of aluminum nano-grating with a period of ~118 nm, a linewidth of ~ 40 nm, and a space of ~ 78 nm. Fig. 8(b) shows a zoom-in view. It is seen that high quality aluminum nanowire grids with 40 nm linewidth and a half-pitch of ~ 59 nm were achieved successfully. In general, the 40 nm wide aluminum nanowires are straight and smooth, although some degree of linewidth variation exists. The linewidth variation is caused mainly by non-uniformity and roughness of the photoresist exposure in the interference lithography process. Fig. 8(c) shows a cross-section SEM photograph of the aluminum nanowire grids. It is seen that 40-nm-wide aluminum nanowires with an excellent profile and over 5:1 aspect-ratio were achieved.

For optical measurement, we used a spectrometer measurement system (Axometrics) based on a lamp covering from 300 nm to 1100 nm. All the measurements were performed at close to normal incidence. Fig. 9 shows measured spectral performance for transmission mode (TM) and extinction ratio for a broad wavelength range from 300 nm (UV) to 900 nm (IR). In the visible to near IR wavelength, 430 nm to 900 nm, it is seen that a flat transmittance of 85% to 91% along

with an extremely high extinction ratio of 40 dB (10,000:1) to 48 (50,000:1) dB were achieved. Compared to the simulation result, the experimental values of the transmittance and extinction ratio, particularly the extinction ratio, are slight lower than the simulated result. This is mainly because the simulation assumes aluminum nanowire-grid with perfect linewidth, shape, smoothness, surface condition (i.e., no oxidization) and material property.

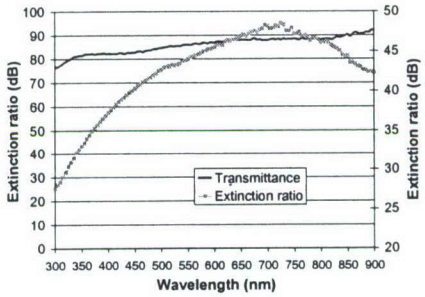

Fig. 9 shows measured spectral optical performance for transmission mode (TM) and extinction ratio at a normal incidence for a broad wavelength range from 300 nm (UV) to 900 nm (IR).

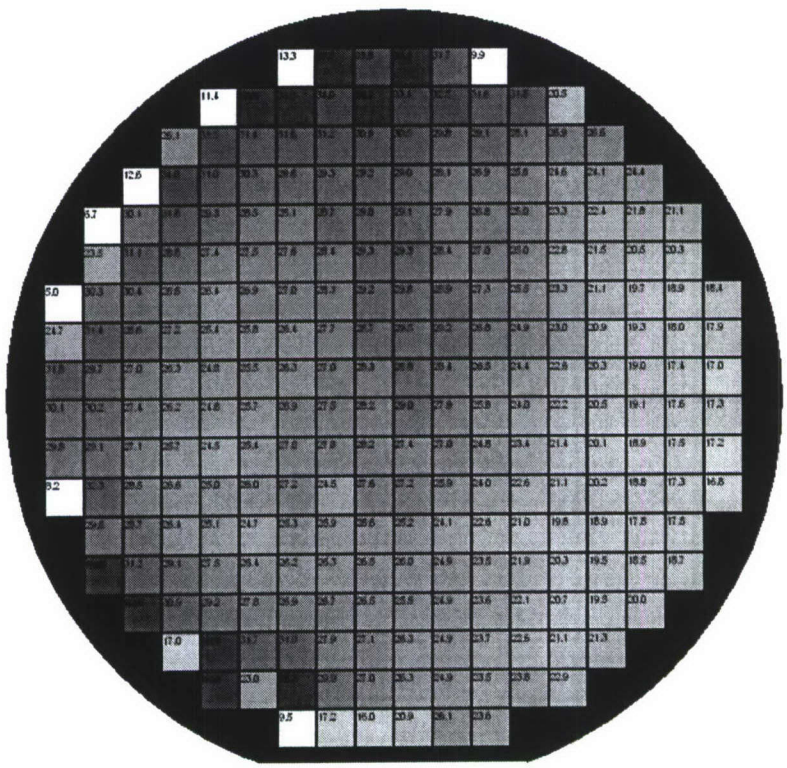

Fig. 10 shows the wafer mapping result for the 100-mm wafer. The extinction ratio at 300 nm was measured for the whole wafer.

The performance at deep ultraviolet wavelength was measured using both 300 nm light from a lamp and the 266 nm laser. Fig. 10 shows the wafer mapping result for the 100-mm wafer. The extinction ratio at 300 nm was measured for the whole wafer. It is seen a relative uniform performance was achieved across the whole 100-mm diameter wafer. The average extinction ratio at 300 nm is 26 dB (~ 400:1) with a distribution of +/- 5 dB. At 266 nm, a transmittance of 65% and extinction ratio of ~ 23 dB (~ 200:1) was measured.

3.3 Nanowire-grid visible polarizer directly on PET plastic substrate

The cost to make the nanowire-grid polarizers reported above is tied to the semiconductor fabrication method, such as reactive ion etching. Fundamentally, the nano-optical wafers fabricated by the semiconductor microlithography method have a much high unit m^2 cost, compared to the optical films made by chemical industrial method such as web-to-web fabrication.

In this work, we aim to make nanowire-grid polarizer directly onto plastic substrates. The purpose of this study is to bridge the previously mentioned semiconductor microlithography method with the future preferred web-to-web method. We will avoid using the microlithography method such as reactive ion etching. To do this, we have to directly imprint the nanowire grating onto (or into) the plastic substrate.

The processes of the plastic visible polarizer fabrication in this study include 1) plastic substrate preparation; 2) mold making; 3) nano-imprint pattern formation and 4) Al deposition.

We started the process with a plastic substrate, polyethylene terephthalate (PET), with 0.25mm thick. The PET sheet was then cut into 100mm diameter wafer size to match the size of the molds used in our process. A UV-curable imprint resist layer was spun coated on top of the PET and the thickness of the resist was controlled to about 200nm. The adhesion between PET substrate and the UV-curable imprint resist is excellent, so the substrate is transparent and flexible. The molds used in the study are in 117nm and 150nm period respectively. They were made by interference lithography. The grating patterns are uniform over whole wafer (100mm diameter). 150nm pitch grating molds were made by interference exposure in air directly, while 117nm pitch grating molds were exposed by immersing the wafer in water. After the gratings patterns were formed in the photoresist, plasma dry etching was applied to transfer the pattern into the Quartz substrate. The prepared molds are treated by perfluorotrichlorosilane to ensure the mold separation after nano-imprint process.

Nano-imprint is used to directly imprint nano-grating onto the PET substrate. 300psi pressure was applied. The pressure is to ensure the uniform contact between mold and substrate. After the resist is deformed by the mold, UV light is shined to cure the resist to solidify the replicated structures on substrate. After mold releasing, 117nm or 150nm pitch polymeric nano-gratings are formed on top of the PET. Once the suitable polymer grating is achieved, Al is coated on the polymer sidewalls with a certain angle as schematically shown in figure 11. Al depth (h), thickness (t) and line width (w) can be controlled and optimized to achieve good optical performances.

Optical performances, such as maximum transmittance (Tmax) and minimum transmittance (Tmin), are measured by wavelength scan (from 400nm to 900nm) and wafer mapping with fixed light wavelengths (450 or 550 or 650nm). The extinction ratio (Er) is calculated from the ratio of Tmax and Tmin.

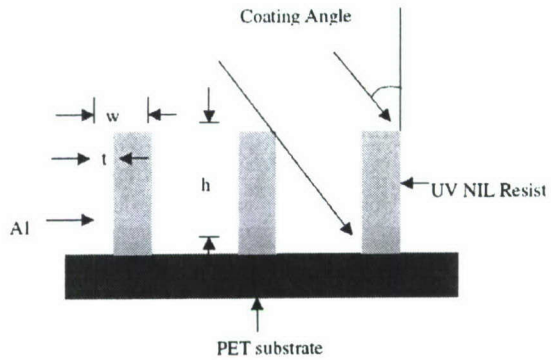

Fig. 11 Al nanowire-grid polarizer directly onto PET substrate.

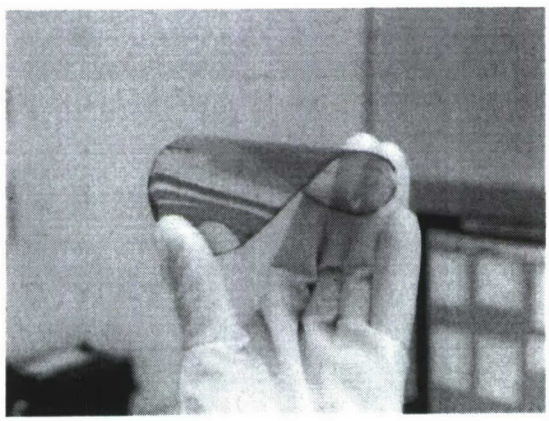

Fig. 12 Flexible nanowire-grid polarizer on PET substrate

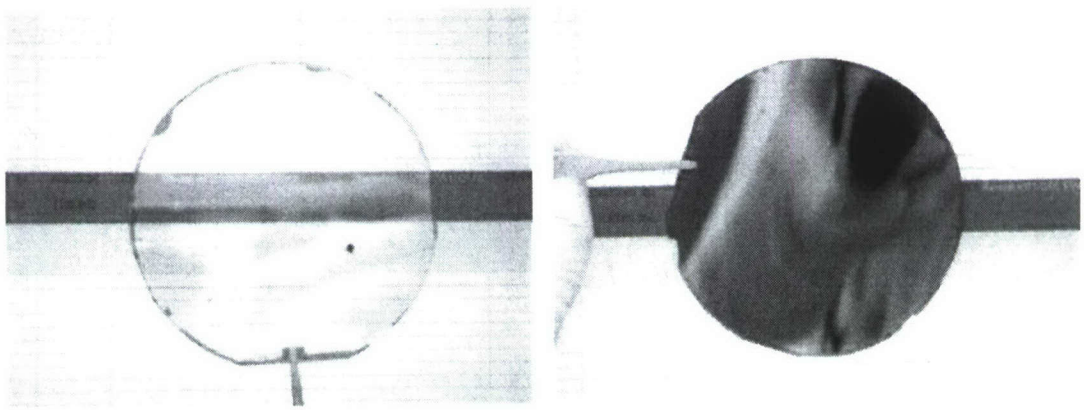

Fig. 13 Optical performance demonstration of the PET nanowire-grid polarizer in front of a LCD screen of a notebook computer: pass state (a) and block state (b).

The fabricated grating and the final plastic wire-grid visible polarizer are shown schematically in Figure 11. The grating heights are controlled in 200nm, while the line width is varied from 40nm to 90nm on different wafers. The Al is shadow coated on the grating sidewall with an oblique angle by e-beam evaporation. A variety of Al line width, depth and thickness have been studied to optimize the optical performances. Figure 12 and Figure 13 illustrates the flexibility of the plastic WGP and its polarizer effect. The polarization and extinction ratio of the selected wafer at 550nm are shown in Figure 14.

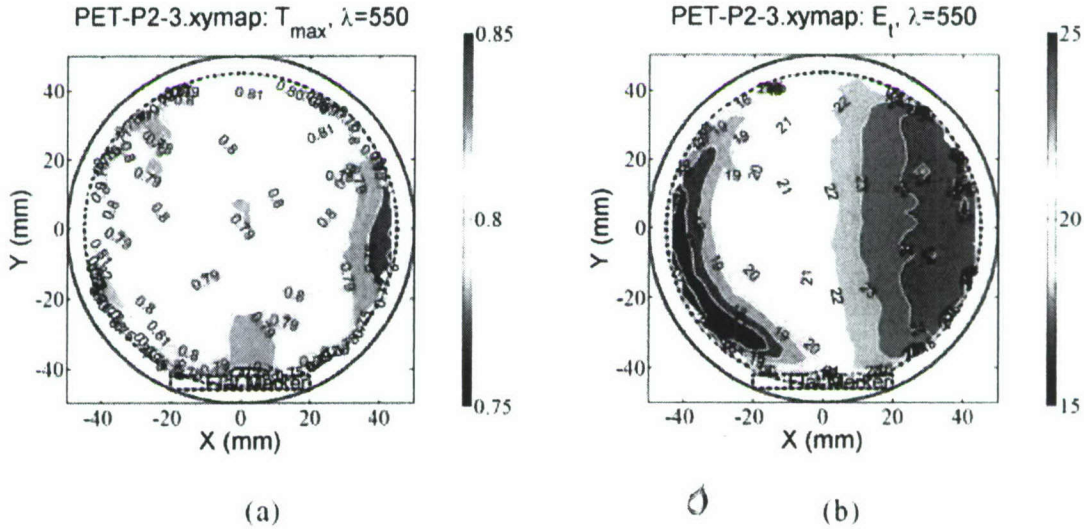

Fig. 14 PET polarizer wafer performance mapping for transmittance (a) and extinction ration in dB (b) at 550 nm of wavelength.

Sub-wavelength optical devices are based on nano-structures, so their optical performance is determined by the geometry of the structures. For Al based WGP in this study, our discussion will be focused on the grating periods (117nm and 150nm), grating line width, Al coating depth and thickness. Grating period is the first issue to be addressed. Simulation has indicated that the grating period for visible WGP must be less than 150nm. For getting better performances, smaller period gratings (~100nm) are preferred. Therefore, 150nm and 117nm grating are fabricated for the plastic visible WGPs in this study. For comparison purpose, the geometric structures are kept same (200nm in depth and 35nm in width) for both 150nm and 117nm periods gratings. Same amount of Al (36nm) is deposited at the same angle (35degree) on both period gratings. SEM top view (Figure 15) shows that the grating widths after Al coating are all in ~50nm range for both gratings. 117nm period wafer shows much higher pattern density compared to the 150nm period wafer. Tmax and Er are measured to illustrate the effect of grating period to the performance of WGPs. As expected, both Tmax and Er are improved by reducing the grating period from 150nm to 117nm as shown in figure 16. Er seems more sensitive to the grating period compared to the Tmax. Clearly, small period grating structure is crucial to achieve better performances for the WGPs, especially in the visible and even shorter wavelengths.

Besides the grating period, the geometry of the Al grating itself is also important to the performances of WGPs. In this study, the effect of polymer grating line width and the Al coatings on the gratings are studied in detail. For the same period gratings, grating line width is important for the light reflection and transmittance of WGPs. For the study purpose, two different line widths are fabricated by using two molds with different line spacing. The large line spacing mold results

in wide grating while the small line spacing mold results in narrow gratings for WGPs. Oxygen plasma etching is further applied to tune the polymer grating line widths. After the gratings are made, same thickness Al, 36nm, is deposited on both wafers at fixed shadow angle, 40 degree. The final line widths on the two wafers are 100nm and 50nm respectively (figure 17). Tmax of the wafers in different line widths are shown in figure 18.

Clearly, Tmax of 50nm line width wafer is much higher than that of the 100nm line width wafer. This result is in accordance with the principle of WGP. That is, the wider metal will generate the higher reflection to the light and result in lower transmittance. For most application of WGPs, high Tmax and Er are the interests. Therefore narrow gratings are preferred to achieve high Tmax. To our surprise, not only Tmax is increased, Er is also improved by reducing the grating line width (as shown in figure 18). This good Tmax and Er correlation can be attributed to the metal shadow deposition in our process. From the schematic drawing in figure 11, it is easy to see that when the gratings are getting narrower, the line spacing is getting larger, so the Al is going deeper on the sidewall. From optical performance point of view, the deeper Al favors higher Er while the narrower finger favors higher Tmax. Therefore, reducing line width can improve Tmax and Er simultaneously. From the above discussion, it has been noticed that the Al depth on grating sidewall is important to the optical performance of WGP, in addition to the grating period and line width. To study the Al depth effect in detail, different Al depth on the sidewall is deposited by changing the Al shadow angle. As the shadow angle is varied from small to large, the deposition depth is changed from deep to shallow. The Al depth on the sidewall can be calculated by the geometry structure of the gratings according to figure 11. Generally, for the same grating structure, Al depth coated at 35 degree is deeper than the one coated at 52 degree. The deeper Al corresponds to the thicker Al in WGP device. Therefore the extinction ratio of the WGP is in the order of 35 degree>45 degree> 52 degree (Figure 19).

On the other hand, Tmax is increasing in the same order as Er (Tmax at 35Degree > 45Degree > 52Degree), as shown in figure 20. This is because that the Al is normally more uniformly on the sidewalls and the thickness on grating top is thinner by reducing the shadow angle. The thinner Al on grating top results in higher Tmax. However, if the Al shadow angle is too small, Al will be close to the grating bottom or even touch the bottom. In this study, the coating of Al at 25 degree is close to the grating bottom, so its Tmax starts to drop at short wavelength, as shown in figure 20.

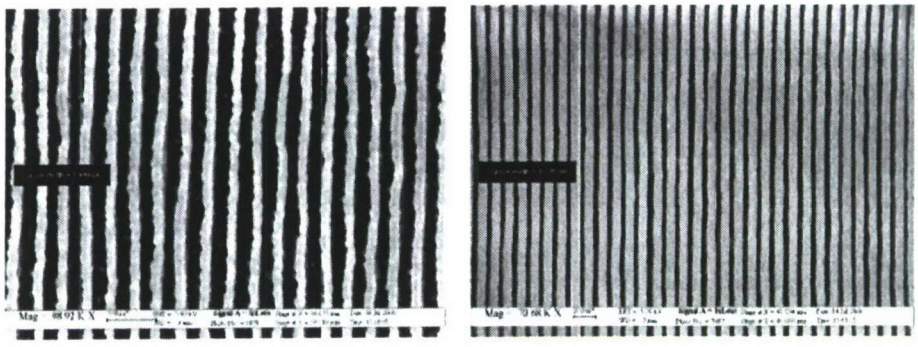

A: 150nm period Al gratings B: 117nm period Al gratings

Fig. 15 SEM of aluminum nanowire-grid on PET with 150 nm period (a) and 117 nm period (b).

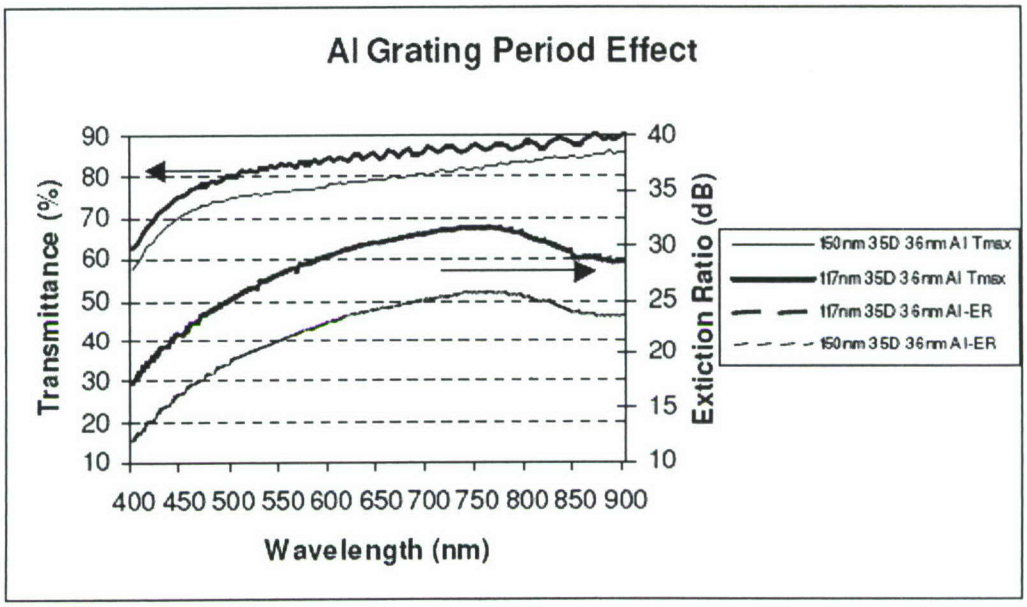

Fig. 16 Grating period effect on the optical performance

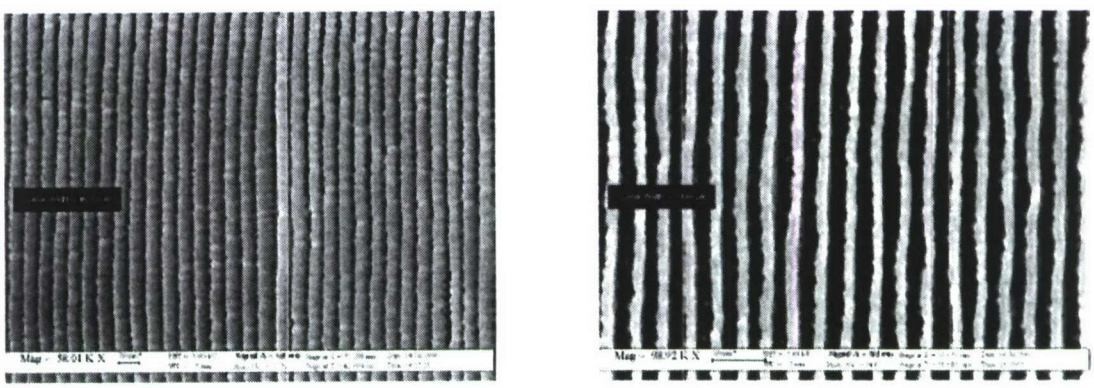

A: ~100nm wide gratings

B: ~50nm gratings

Fig. 17 SEM of aluminum linewidth

From the above discussion, it is interesting to see that Tmax and Er can be improved simultaneously by reducing the grating period, grating line width or Al shadow angle. In addition to those factors, Al thickness is another factor to affect both Tmax and Er. To compare the Al thickness effect, same grating structure is applied for different Al thickness coating. Figure 21 shows the optical performances of the samples with 36nm and 40nm Al respectively. Clearly, by simply increasing the Al thickness, the extinction ratio, Er, of the sample is increased but the Tmax is decreased. In principle, thick Al can improve Er, but the light absorption also increases with the thickness. The light absorption in Al causes the low Tmax.

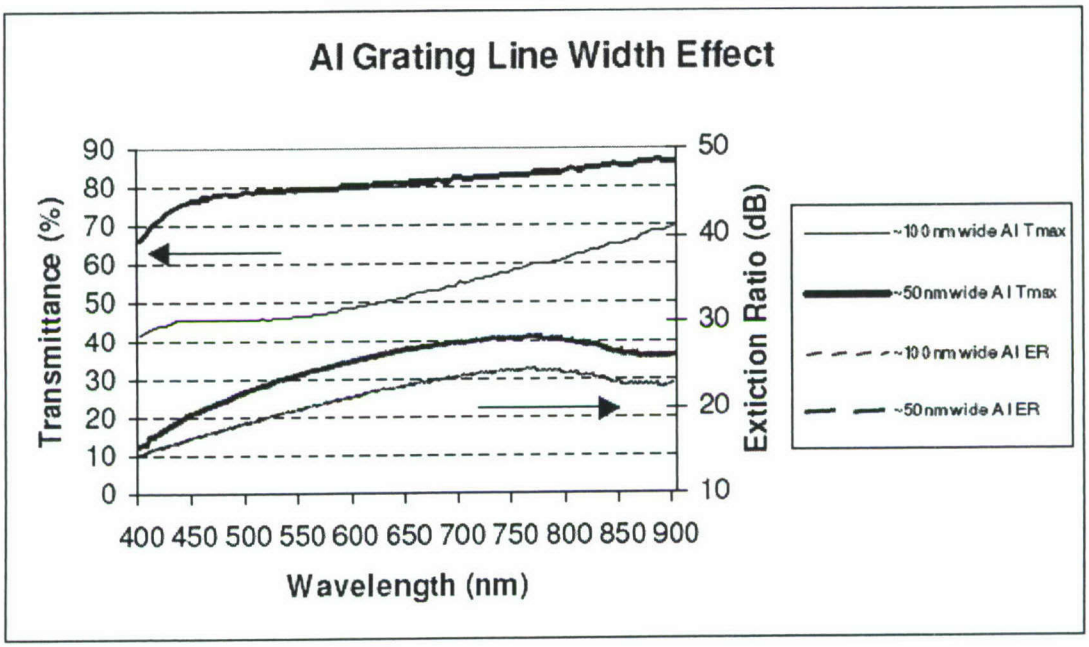

Fig. 18 Maximal transmittance and extinction ratio for the two selected wafer samples

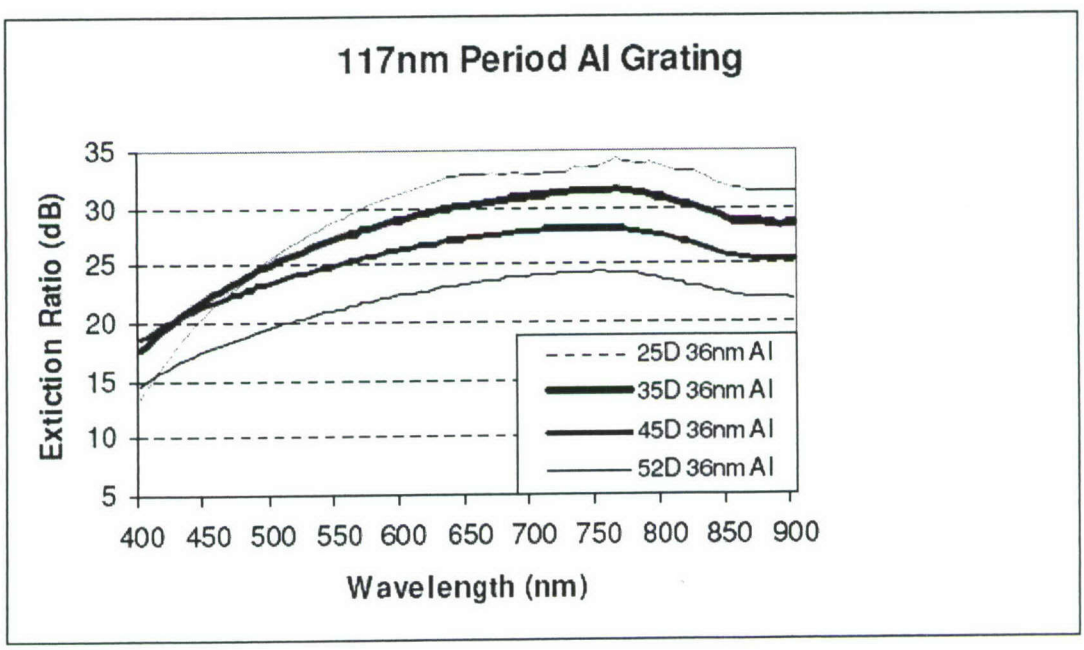

Fig. 19 Extinction ratio for different deposition angles

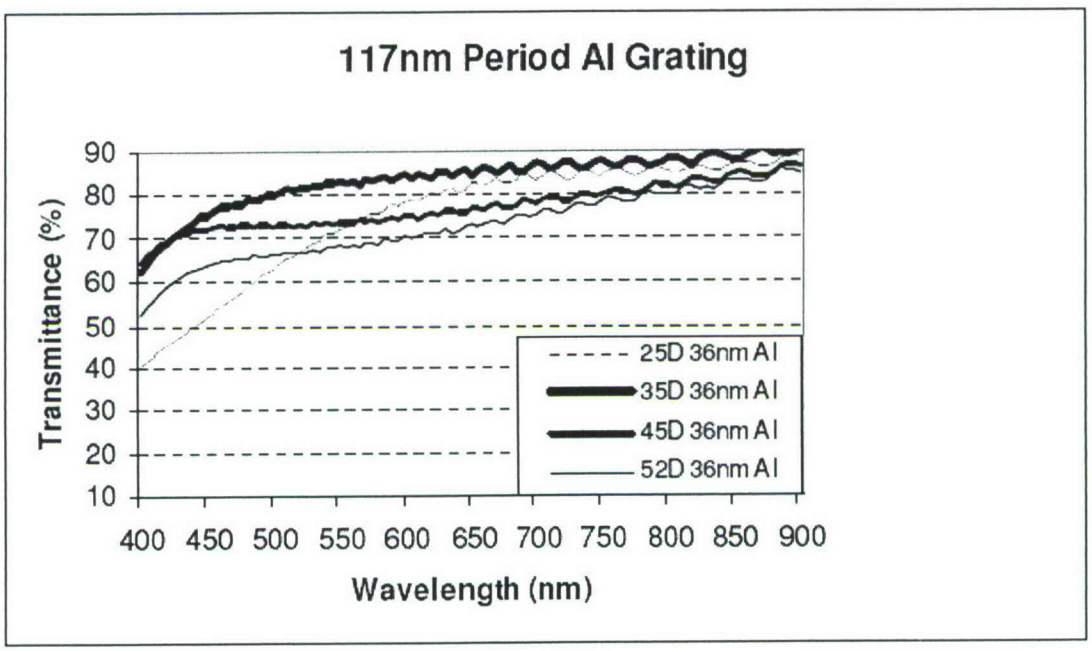

Fig. 20 Transmittance of the polarizer with different Al deposition angles

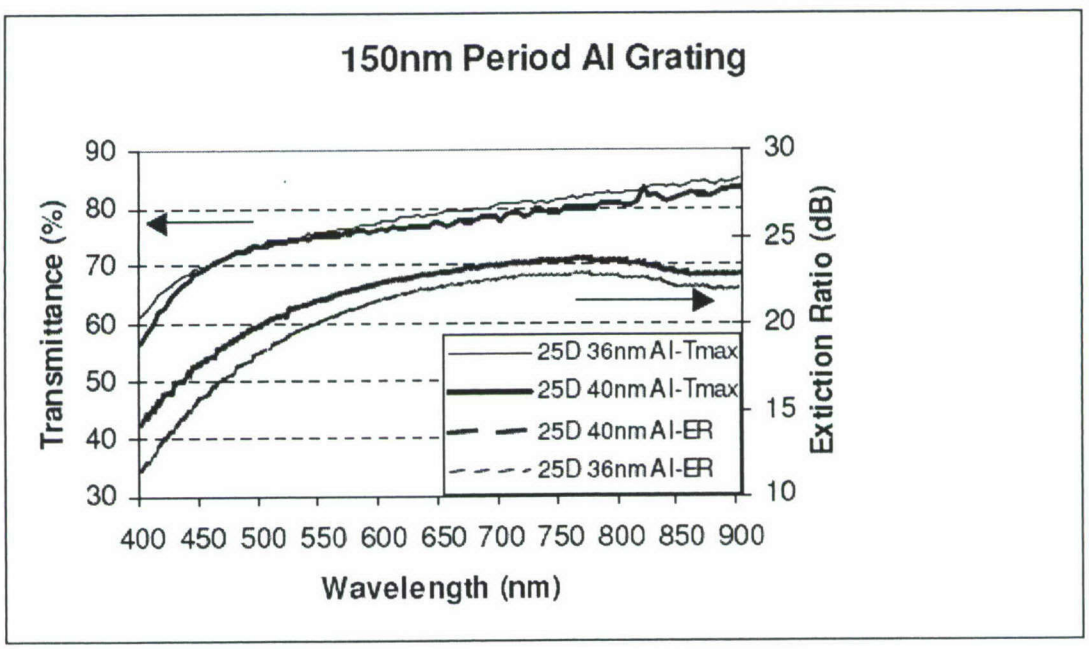

Fig. 21 Al thickness effect on the optical performance

Over all, by reducing the grating period (from 150 to 117nm), and adjusting the grating finger width, Al deposition depth and thickness, we can tune the optical performances of the samples. Excellent transmittance (~80%) and high optical contrast (~20dB) are demonstrated on the large flexible plastic substrates.

3.4 Nanowire-grid waveplate

Waveplate is one key subcomponent for the integrated nano-optical polarimeter. In this work, an integrated half-wave plate (HWP) for a center wavelength of 405 nm is achieved by integrating two fully-filled and planarized nano-grating quarter-wave plate layers monolithically. We report optical devices based on monolithic integration of multiple nano-structured optical functional layers. Ultraviolet (UV)-nanoimprint lithography along with thin-film deposition, high aspect-ratio reactive ion etching (RIE) and trench-filling technologies were used in fabrication and integration of individual nano-structured optical functional layers. Structures with sub-50 nm linewidth were required in order to achieve good optical performance in the near-UV and visible wavelengths.

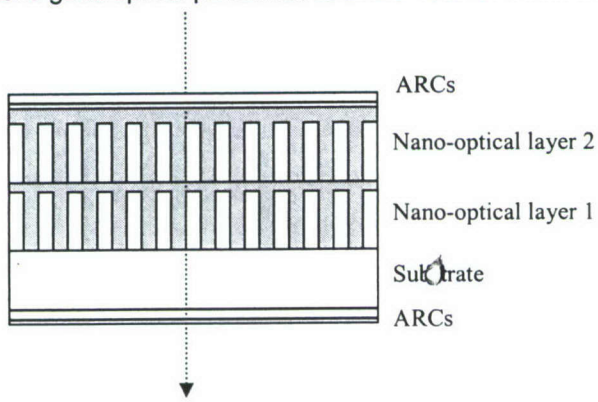

Fig. 22 Schematic of a two-layer monolithically integrated nano-optical device. Each individual nano-grating layer is fully trench filled and planarized.

It is well understood that sub-wavelength dielectric and metal nano-gratings are optically anisotropic. The structure induced birefringence has been utilized to make wave plates, as well as polarizers, at visible and near-infrared (NIR) wavelengths. Air channels have been routinely used as the lower index media in the nano-gratings. The problems associated with air channels in a nano-structured optical device are multi-fold: (a) the air-channeled structure could cause reliability issues. The water vapor attracted into the air channels could change device's optical performance, as well as its long-term reliability; (b) the air-channeled structure, particularly used as a underneath structure, can make the device mechanically weak. It prevents integration (i.e., stacking) of more nano-structured layers on top of the air-channeled layer. Here we overcame those issues with a new design based on inorganic fully trench-filled and planarized nano-grating structures, as schematically shown in Fig. 22. Rigorous coupled-wave analysis was used to design the integrated nano-optical devices.

One-dimensional sub-wavelength grating made of homogeneous materials breaks in-plane symmetry of the material which leads to artificial birefringence property, i.e., form-birefringence. For a wave plate of retardation φ at wavelength λ, the required grating depth t_G for a grating of

period Λ and a duty cycle α, is $t_G = [\varphi/2\pi]\cdot(\lambda/\Delta n)$, where Δn is the magnitude of the birefringence. For $\alpha \approx 0.5$, $\Delta n \approx (n_H - n_L)^2/[2(n_H^2 + n_L^2)]^{1/2}$, where n_H and n_L are the high and low refractive indices of the grating materials, respectively. Δn decreases very quickly as the index n_L increases from 1 (i.e., air) to approach n_H. On the other hand, the average refractive index of gratings increases, and the grating period $\Lambda << \lambda/[(n_H^2 + n_L^2)/2]^{1/2}$. This demands the aspect ratios of the gratings γ to increase at speed faster than $(\varphi/\pi)\cdot(n_H^2 + n_L^2)/(n_H - n_L)^2$. For gratings composed of Ta_2O_5 and SiO_2, we calculated from a rigorous coupled wave analysis (RCWA) that $\Lambda \leq 160$nm for QWPs and HWPs working around 405 nm, and $\gamma \approx 8$ and 16 for QWPs and HWPs, respectively.

To realize the design structure described above, a 100 mm-diameter glass (e.g., BK7 or C1737F) wafer deposited with a thick (~ 1 μm) SiO_2 was spin-coated with a thin layer (~ 180 nm) of a UV curable resist. After baking, the resist was imprinted with a grating mold having a period of 145 nm and depth of about 110 nm, and a grating linewidth of about 100 nm, by a UV nano-imprint process. The mold consisted of a patterned SiO_2 layer (about 200 nm thick) on a 0.5 mm thick silicon wafer. After imprinting, the deformed UV curable resist was fully cured by exposing to UV light. The mold was then separated from the resist, leaving a mask with a negative pattern of the mold profile. After that, a series of process were used to transfer the pattern into the underneath SiO_2 in order to form the nano-gratings. The width of the final etched SiO_2 grating can be tailored under good process control capability during the pattern transfer process as discussed in our previous publications. The trenches of the nano-gratings were filled with various optical materials or nano-laminate materials by atomic-layer depositions (ALD). The material choices include such as TiO_2, Ta_2O_5, Al_2O_3, HfO_2, and SiO_2, etc. The ALD deposition was performed using a home-made ALD machine.

We find it necessary to use buffer layers under the gratings to minimize reflection losses. Fig. 23 illustrates a QWP designed for center wavelength of 405 nm for Blue-Ray and HD-DVD applications. The other side of the glass substrate (not shown in Fig. 22) is antireflection coated. A ~630 nm thick SiO_2 layer was patterned via reactive ion etching (RIE) with slightly tapered profile. Then the gratings were trench filled and planarized with Ta_2O_5 in an atomic layer deposition (ALD) chamber. The coating process is highly conformal and precisely controlled on thickness and optical dispersion. With 3–layer thin films deposited to reduce the reflection, we obtained a QWP with a phase retardance of 90 +/- 7 degrees and transmittance of >90% across the whole 100 mm diameter at 405 nm.

We further took advantage of the planarized structure. A second group of buffer layers with another 630nm SiO_2 were e-beam evaporated with argon-ion assisted deposited (IAD) on top of the first layer grating. A second UV-nanoimprint lithography, RIE and ALD processes brought the structure to a HWP at 405 nm, as shown in Fig. 23. Slightly modified 3-layer overcoat gave ~88% transmittance. Further optimization of the coatings would improve this value to >95%. The retardation map at 405 nm of the 100-mm diameter wafer is shown in Fig. 25. We clearly have a 180~187 deg phase plate. The spectral performance of the HWP is shown in Fig. 26. The wavefront distortion (WFD) of the QWPs and HWPs by using a Zygo/GPI interferometer are <20 mλ rms at 10 mm-diameter aperture. Both the QWP and HWP can be further integrated with the other micro-optics, for example, in an optical pickup head, for data storage applications. Based on this method, we design more complex multi-layer integrated nano-optical devices. With more grating layers, we expect to have more functions integrated together.

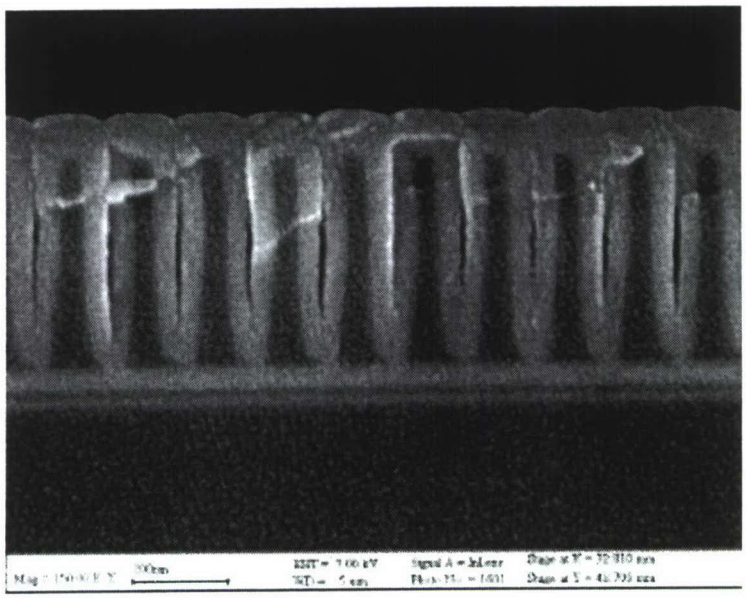

Fig. 23 A cross-sectional SEM photograph of a quarter-wave plate with fully trench filled nano-grating structure. The nano-grating has a period of ~ 145 nm, a linewidth of ~ 50 nm and a depth of ~ 630 nm.

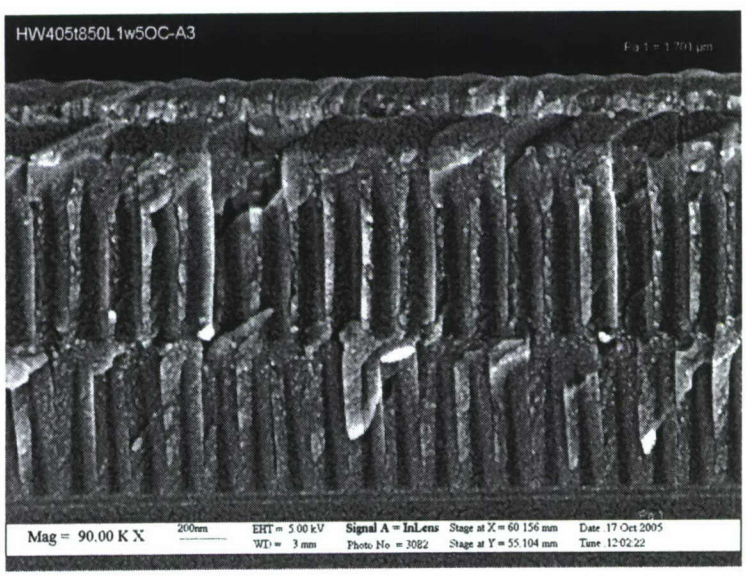

Fig. 24 A cross-sectional SEM photograph of a monolithically two-layer integrated half-wave plate with two fully trench filled nano-structure grating layers.

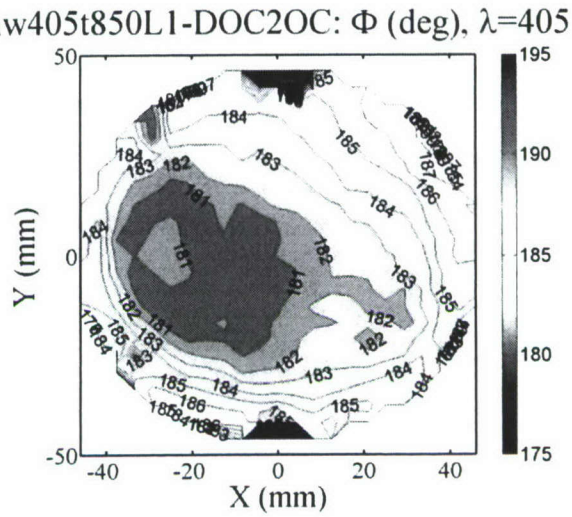

Fig. 25 Phase retardance performance of a 100 mm-in-diameter wafer. This performance is corresponding to the structure as shown in Fig. 24, i.e., with an integrated half-wave plate with two-layer integrated nano-structured gratings.

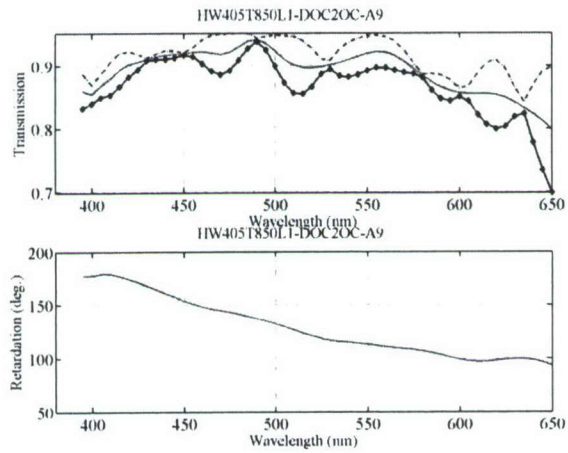

Fig. 26 Optical performance of the monolithically integrated half-wave plate.

For future improvement on reducing possible UV absorption and aging, a larger band material such as TiO_2 is preferred for trench filling compared to Ta_2O_5. To match the refractive index of Ta_2O_5, a nano-composite material of TiO_2:SiO_2 with certain ratio can be used.

3.5 Monolithically integrated circular polarizer based on stacking two nano-grating layers

The finished aluminum nanowire-grids are very susceptible to surface scratches and can be easily damaged with a soft cloth. Also, the exposed aluminum nanowires have a reliability concern, particularly in a high-temperature and high-humidity environment. Considering the above reasons and the planarization requirement for integration needs, the aluminum nanowires were trench-filled with SiO_2 and thus buried into SiO_2. Fig. 27(a) shows a cross-sectional SEM photograph of the buried aluminum nanowires. We used an atomic-layer deposition (ALD) technique for the trench-filling and bury. This technique simultaneously works as a planarization process. It is seen that a very small surface ripple (<20 nm peak to peak) exists from the conformal deposition nature of the ALD process.

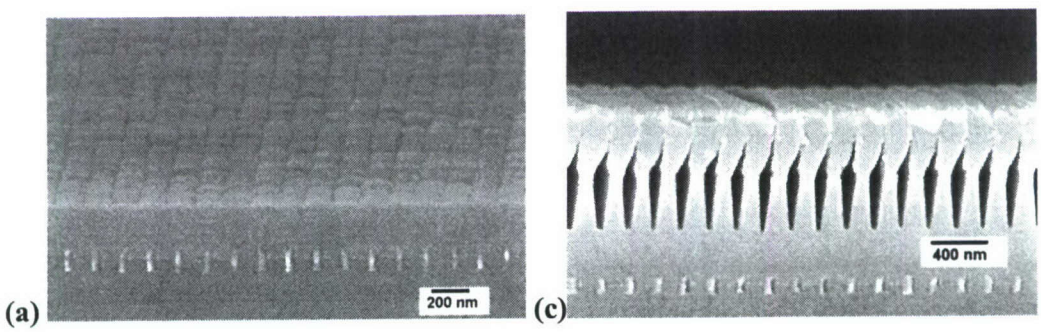

Fig. 27(a) A cross-sectional SEM photograph of the buried aluminum nanowires. Fig. 27(b) A cross-sectional SEM photograph of a finished fully integrated circular polarizer.

The finished surface of the buried aluminum nanowire grid polarizer has hardness close to that of a glass surface. The 20-nm surface ripple is flat enough for further processing for integration. A broadband high-performance visible quarter waveplate was then fabricated. We have achieved a standalone visible quarter waveplate centered at a wavelength of 650 nm, based on a 200-nm period silicon nitride grating. Both a very high transmittance of >98% and a very uniform phase retardation distribution of 90° ± 2° across a 100-mm diameter wafer were achieved. To integrate the quarter waveplate monolithically, a silicon-nitride film of ~650 nm was then deposited onto the filled polarizer surface by plasma enhanced chemical vapor deposition (PECVD). We then applied the second UV-nano-imprint process to pattern a 200-nm period resist pattern on top of the nitride layer. The second nano-grating, which determines the optical axis of the quarter waveplate, was aligned to be oriented at 45° from the pass direction of the aluminum nanowire grid polarizer underneath. The nitride layer was then deep etched by a CHF_3 reactive ion etching (RIE). And finally, overcoating layers as ARCs were deposited on top of the nitride gratings by an oblique e-beam deposition process. Fig. 27(b) shows a cross-sectional SEM photograph of a fully finished integrated circular polarizer.

The finished monolithically integrated visible circular polarizer achieved very good performance. Optical performance of the circular polarizer was characterized by using a linearly polarized incident light with a wavelength of 650 nm. Fig. 28 shows the measured circularity of the final integrated circular polarizer with incident light polarized parallel to pass the direction of the nanowire grid polarizer. A circularly polarized light was generated with a high transmittance of >80%.

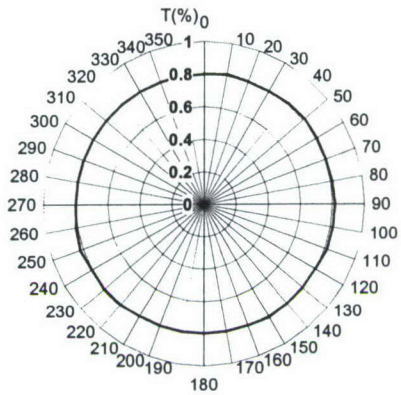

Fig. 28 The measured circularity of the final integrated circular polarizer (Fig. 27(b)) with incident light polarized parallel to the pass direction of the nanowire grid polarizer.

4. Report on pixilated nanowire-grid polarizer and wave plate

We have made significant progress for all the necessary nano-optical sub-components which are needed for making the final monolithically integrated nano-optical polarimeter.

The next is concentrated on making pixel array for those sub-component function layers, they are, pixilated polarizer, pixilated waveplate and "pixilated" micro-lens array (see section 4). Pixilation process and technology are also part of the key processes and technologies enabled the final integrated polarimeter.

We have successfully demonstrated the first pixilated nanowire-grid polarizer with aluminum nanowire grids of 150 nm period and 70 nm linewidth. The size of the individual pixel is about 10 microns. The design of such nanowire-grid polarizer is based on our previous experience and knowledge from making large-area such polarizer device as described above.

The key step of making such pixilated polarizer is making the nanoimprint mold. We have relied on a commercial e-beam system (Photronics Inc.) to write the pixilated nano-grating mold. The mold is made of fused silica substrate of 1.7 mm thickness. The pixel array has a repetitive cell which contains four sub-pixel. Each sub-pixel has a size of 10 micron. Between the four sub-pixels, the grating orientations cover 0 degree, 90 degree, 45 degree and 135 degree. The pixel pattern is etched into the fused silica substrate with a depth of about 100 nm. The finished mold was treated with mold release agent before used for nanoimprinting.

For making the pixilated polarizer, we started with a glass substrate which is coated with 150 nm thick of Al and 20 nm thick of SiO2 for etching hardmask. A thin layer of home-prepared UV-curable nanoimprint resist (OP133) with a thickness of ~ 150 nm was then spun coated on. The UV-nanoimprint process was then used to form the resist pattern.

The whole UV-nanoimprint process took only about few minutes. There was a continuous and uniform resist residual layer with a thickness of about 100 nm underneath the resist lines. In order to expose the underneath SiO_2 layer between the patterned resist lines, a blank oxygen reactive ion etching (RIE) (3 mtorr, 50 W, 4 sccm) with varied etching depths was conducted in order to achieve different resist linewidths prior to etching of the SiO_2 hard mask. After that, an RIE process with CHF_3 (5 mtorr, 100 W, 10 sccm) was used to etch 20 nm SiO_2 with the polymer resist line as masks. Finally, a chlorine-based RIE process (60 sccm BCl_3 and 50 sccm Cl_2 at 5 mtorr) was used to etch aluminum layer into aluminum nanowire-grid by using the patterned SiO_2 as etching hard mask. The final linewidth of the aluminum wires is determined by the linewidth of the SiO_2 hard mask, which can be controlled by the linewidth of the mold and the blank oxygen RIE etch depth.

Figure 29 shows the SEM picture of a repetitive unit with four sub-pixels. This is the top view of the finished final pixilated polarizer.

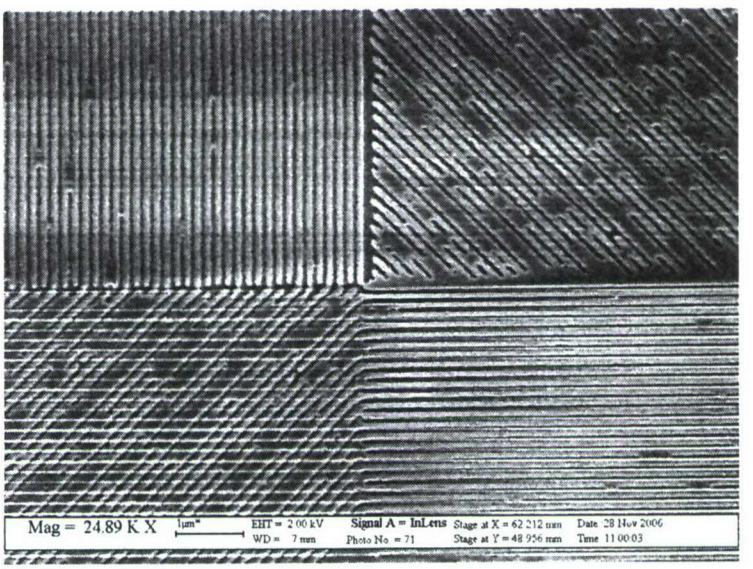

Fig. 29 SEM top view of a repetitive unit of the pixilated nanowire-grid polarizer. The unit contains four sub-pixels, and each of the sub-pixel has a size of 10 micron x 10 micron. The period of the nanowire-grid polarizer is about 150 nm.

It is clear that the 0 degree and the 90 degree sub-pixels have better defined pattern than the 45 degree and the 135 degree ones. This is mainly caused by the quality of the e-beam made imprint mold. The commercial e-beam system at Photronics Inc. has some problem to generate perfect e-beam writing patterns for 45 degree and 135 degree orientations. Currently, we are working with other commercial e-beam houses to improve the quality of the original imprint molds for the pixilated patterns.

The major challenge for the state-of-the-art e-beam system is to write such dense line patterns with a linewidth of 70 nm or below and spacing of 70 nm or below.

Figure 30 shows the AFM (atomic force microscope) image of the same repetitive unit of the pixilated nanowire-grid polarizer as shown in Fig. 29.

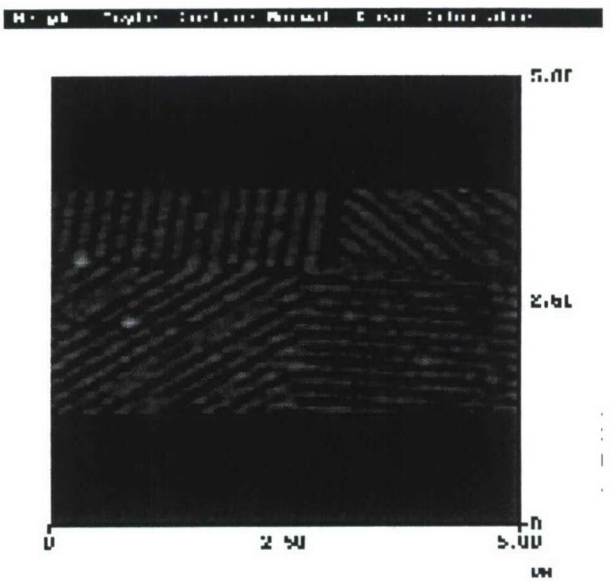

Figure 30 shows the AFM (atomic force microscope) image of the same repetitive unit of the pixilated nanowire-grid polarizer as shown in Fig. 29.

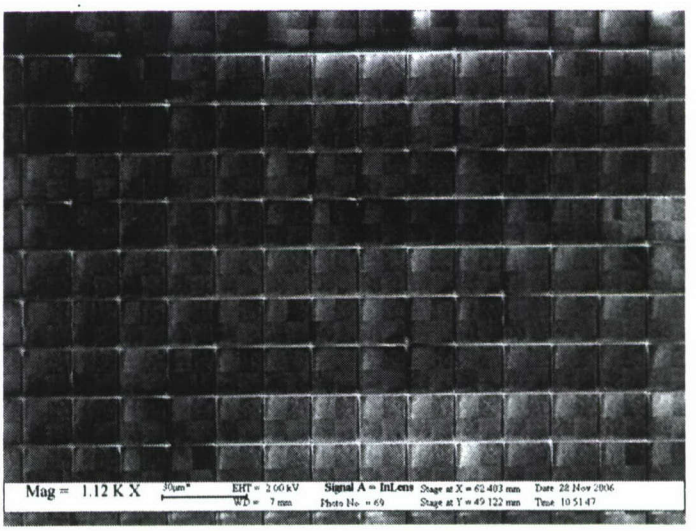

Figure 31 SEM top view of a larger area of the pixilated polarizer.

Figure 31 shows SEM top view of the pixilated polarizer for a larger area of about over 100 microns x 100 microns.

We continued to build nanowire-grid pixilated waveplate. Historically, pixilated waveplate or retarder was never made. The main reasons are following: (1) the conventional technique based on crystal like quartz for waveplate/retarder is not able to build pixilated waveplate array (except by manually assembling diced crystal waveplate chips which can not be too small); (2) there is same problem with the conventional technique for waveplate/retarder based on stretched polymer technique. Based on our opinion, the nano-optical waveplate/retarder technology based on nano-grating created form birefringence is the only creditable solution. In addition, the nano-trench filling technology discussed previously in the first report further enable us to fabricate the pixilated retarder/waveplate with a fully trench filled structure. In other words, such pixilated fully nano-trench-filled retarder forms a planar surface which makes the monolithic integration of the pixilated retarder with other nano-optical functional layers, such as a pixilated polarizer layer, feasible now for the first time.

Fig. 32 shows the fabrication sequence for fabrication of such pixilated retarder/waveplate.

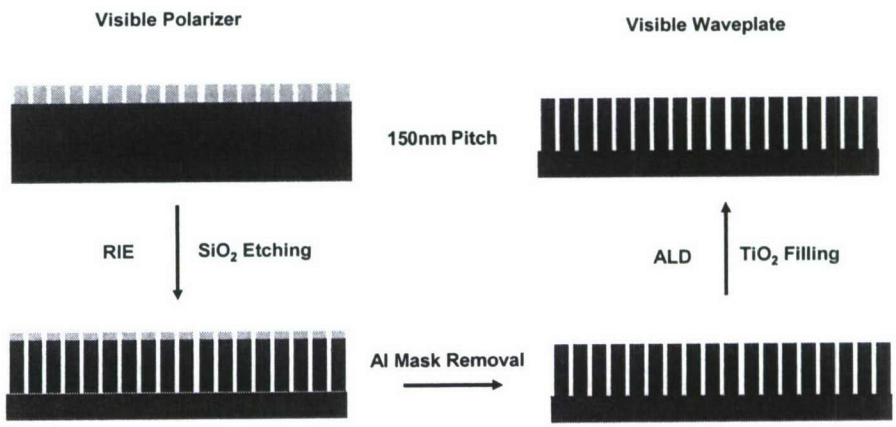

Fig. 32 Fabrication sequence for forming trench-filled waveplate/retarder.

To fabricate the pixilated retarder, we started with a pixilated nanowire-grid polarizer structure. Basically, we use the aluminum wires from the pixilated nanowire-grid polarizer as the hard etching mask. In current case, the pixilated aluminum wire array has a period of about 150 nm with a duty cycle of about 50%. The depth of the aluminum wire is about 120 nm. The substrate used here is a fused silica substrate. A RIE process (5 mtorr, 10 sccm CHF3, 0.5 sccm O2, 150W) was used to etch the fused silica (SiO2) with the aluminum as hard mask. As shown in Fig. 33, an etching depth of ~ 600 nm was achieved with a good etching profile. After etching, the aluminum mask was removed by wet KOH etching. Then, the atomic layer deposition process was used to fully fill the nano-trenches with a high index material, i.e., TiO2. Atomic layer deposition (ALD) is a

process for depositing highly uniform and conformal thin films by alternating exposures of a surface to vapors of two chemical reactants. ALD was applied in this work to fill high aspect ratio nano-gratings. The potential for filling with nano-laminate material is one key advantage for using ALD for nano-structure fillings. The ability of dialing the optical properties of the filling materials can significantly enhance our design freedom and process window.

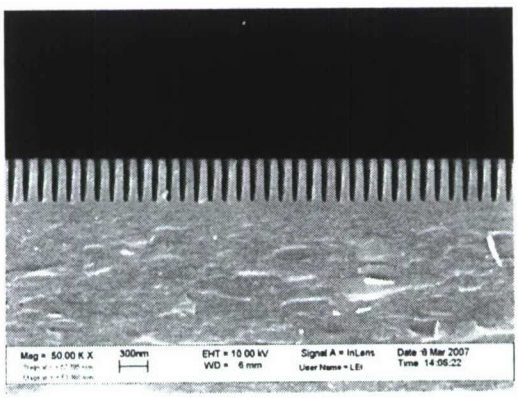

Fig. 33 The SEM photograph of a 600-nm deep nano-grating with a period of 150 nm into fused silica substrate.

The trenches of the gratings were filled with a nano-laminate material composed of TiO_2 and SiO_2. The nano-laminate material was deposited by ALD, which was performed using a home-made ALD machine. Prior to depositing the nano-laminate, the grating wafer was heated to 300°C inside the ALD chamber for about three hours. The chamber was flushed with nitrogen gas, flowed at about 2 SLM, maintaining the chamber pressure at about 0.75 Torr. The TiO_2 precursor was Ti-ethaoxide, which was heated to about 140°C. The SiO_2 precursor was silanol (tris(tert-butoxy)silanol), heated to about 110°C. For both precursors, the reagent used was water, which was maintained at about 13°C. The Ti-ethaoxide and silanol were 99.999% grade purity, obtained from Sigma-Aldrich (St. Louis, MO). The nano-laminate was formed by repeating a cycle in which M monolayers of TiO_2 were deposited, followed by a single monolayer of SiO_2. Depending on the design, M can be varied from 0 (i.e., SiO_2) to over 20 (i.e, close to TiO_2). To deposit a TiO_2 monolayer, water was introduced to the chamber for two seconds, followed by a two second nitrogen purge. Then Ti-ethaoxide was introduced to the chamber, followed by another two second nitrogen purge. SiO_2 monolayers were deposited by introducing water to the ALD chamber for one second, followed by a two second nitrogen purge. Silanol was then introduced for one second. The chamber was then purged for three seconds with nitrogen before the next pulse of reagent. By changing M, the refractive index of the nano-laminate material can be varied in a large range from 1.46 to 2.35. It has been demonstrated that the ALD is able to completely (i.e., void-free) fill gratings with an aspect-ratio greater than 12:1. The trenches of the nano-gratings can also be filled with other optical materials or nano-laminate materials by atomic-layer depositions (ALD). The material choices include such as TiO_2, Ta_2O_5, Al_2O_3, HfO_2, etc.

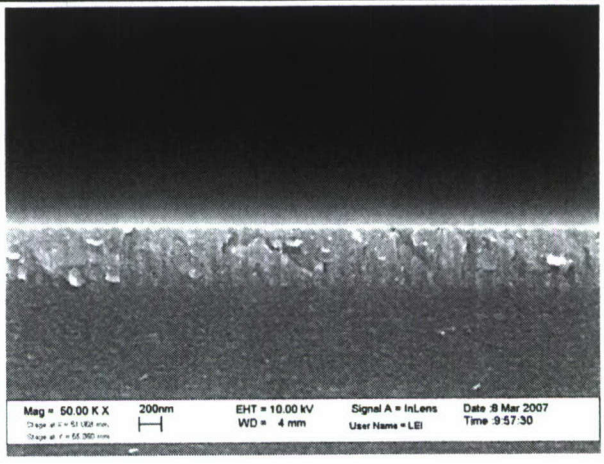

Fig. 34 SEM photograph of a fully trench-filled nano-grating waveplate/retarder.

Fig. 34 shows the cross sectional SEM photo of the fully trench filled nano-grating. From the contrast difference between the nano-gratings, we can clearly see the original fused silica SiO2 part and the filled-in TiO2 part. Due to crystallization, the TiO2 material is much rougher than the SiO2. The reason we used nanolaminated TiO2/SiO2 by laminating a small percentage of SiO2 is to terminate the crystallization of the pure TiO2.

Due to the conformal nature of the trench filling, the top surface of the trench filled retarder shows a very small ripple which is translated from the underneath grating structure. The orientation of the ripple is parallel to the orientation of the original grating. The peak-to-valley depth of this ripple is a function of the depth of the trench fill deposition. Thicker the deposition, smaller is the peak-to-valley of the ripple.

Fig. 35 shows a similar photo but with a borofloat glass substrate rather than the fused silica substrate. The etching characteristic of the borofloat material is a bit difference from the fused silica material as shown by the Fig. 33.

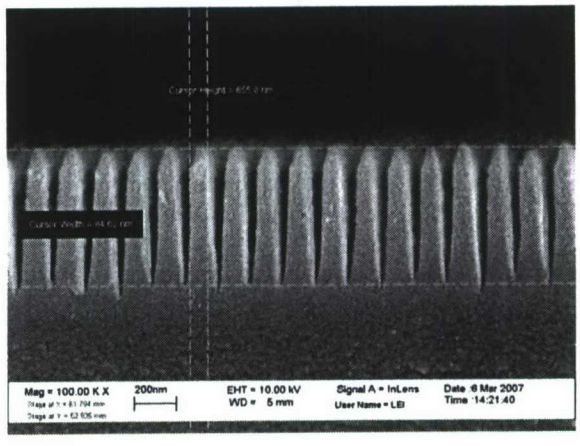

Fig. 35 SEM photograph of a similar nano-grating as shown in Fig. 33 but into a borofloat glass substrate.

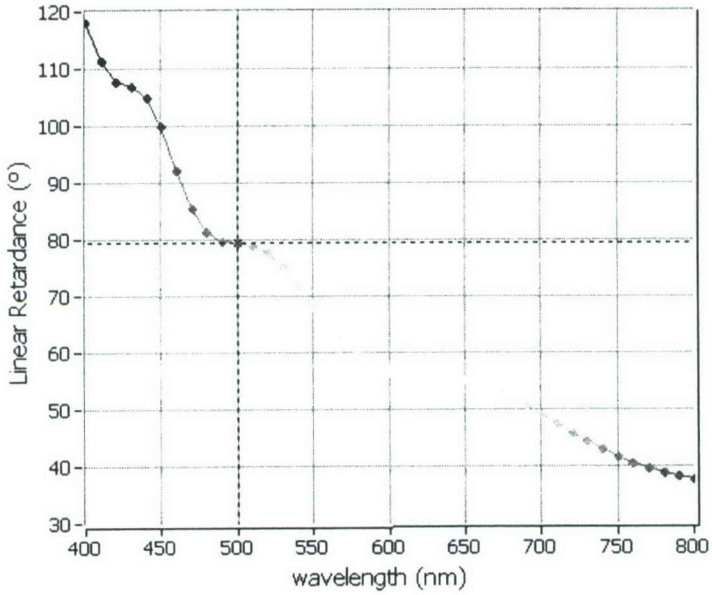

Fig. 36

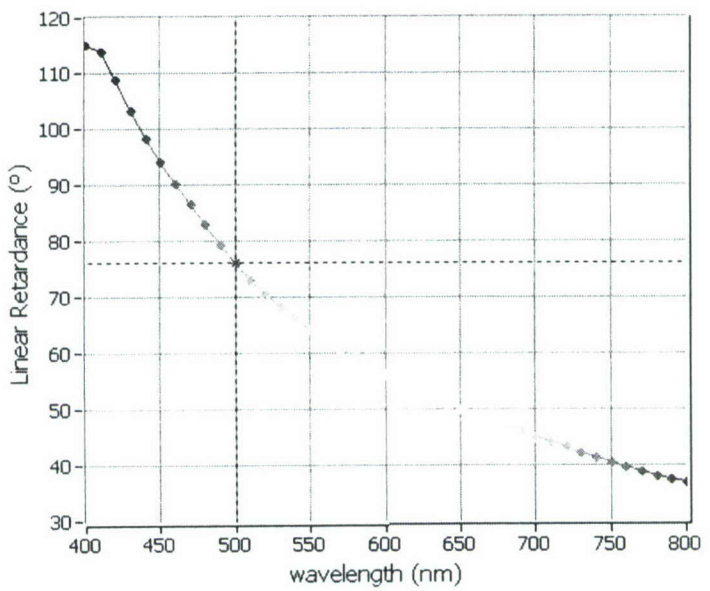

Fig. 37

Fig. 36 and Fig. 37 show the optical retardance measurement result for the non-pixilated waveplate/retarder wafers, one is for fused silica substrate and one is for borofloat substrate.

Fig. 36 and Fig. 37 show the optical retardance measurement result for the non-pixilated waveplate/retarder wafers, one is for fused silica substrate and one is for borofloat

substrate. For both cases, the retarder is almost a quarter-wave plate (90-degree retardance) at wavelength around 450 nm to 500 nm. The dispersion of the retardance is a typically true-zero-order retarder characteristic.

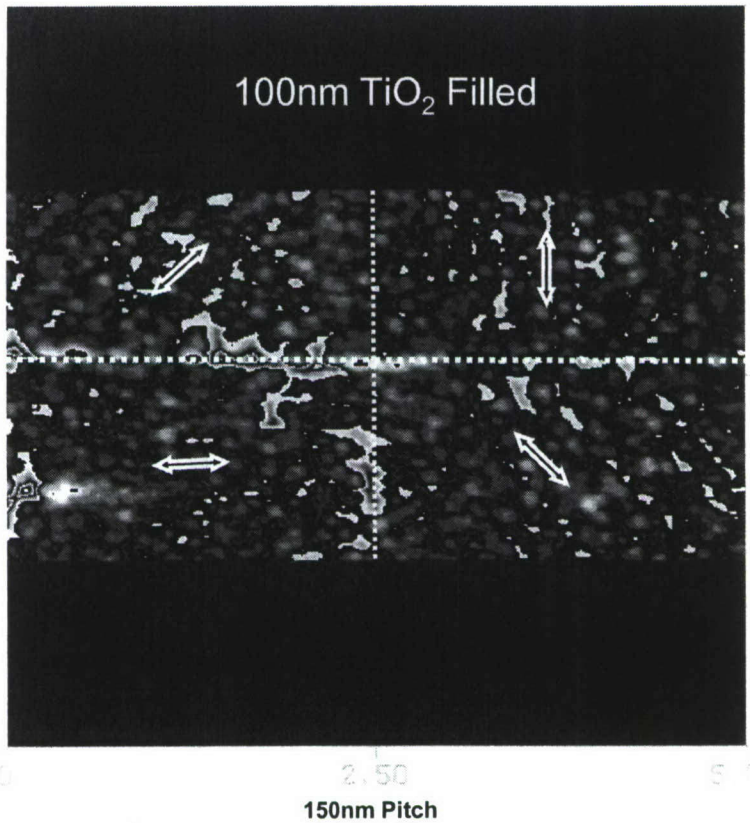

Fig. 38 shows the atomic force microscope (AFM) image of the pixilated trench-filled retarder.

Fig. 38 shows the atomic force microscope (AFM) image of the pixilated trench-filled retarder. The orientation of the each pixilated retarder can be barely seen by looking at the top ripple. We intentionally marked the orientation of each pixilated retarder and the boundary between the pixels.

Fig. 39 shows the optical retardance measurement for the pixilated retarder array. Other than a very weak retardance, we basically did not observe any retarder effect from the pixilated array. Since the test light beam size covers hundreds of the individual retarder pixels, the final test result is actually the average of the retardance from each individual pixel. Therefore, there should be no "macroscopic"-level retardance which matches with the real data.

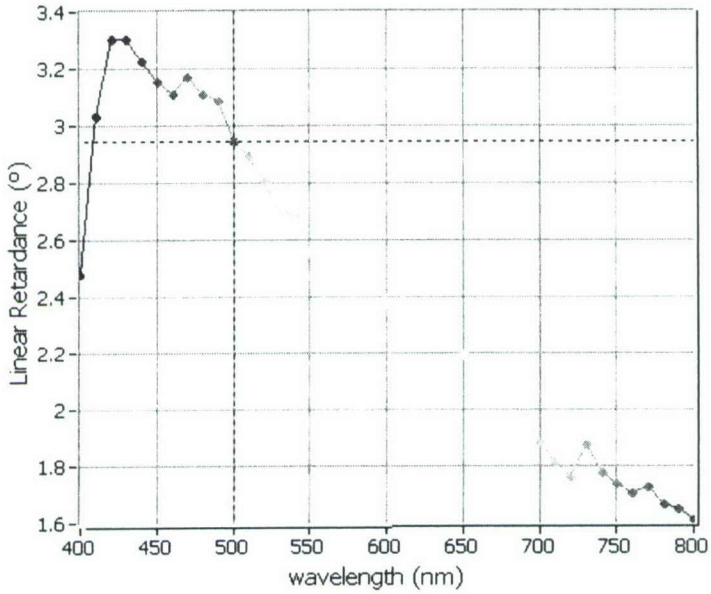

Fig. 39 shows the optical retardance measurement for the pixilated retarder array.

In summary, we have successfully fabricated monolithical pixilated waveplate/retarder array with pixel size down to 10 microns. We believe this was the first monolithic and dielectric pixilated retarder/waveplate which has been ever fabricated.

We are working on building the integrated polarimeter by stacking and aligning the two layers.

5. Progress Report on Developing Continuous Printing with Roller Nanoimprint Lithography (by University of Michigan)

Work performed at UM is focused on constructing an automatic and continuously operated roller imprinting apparatus and exploiting UV curable liquid resist for high speed patterning [3]. We also fabricated wire grid polarizer by using R2RNIL approach.

5.1. Development of Roll-to-roll Nanoimprint Lithography (R2RNIL) Device and Setup

Figure 40 shows the overall configuration of a continuous R2RNIL nanomanufacturing process, which consists of three separate processing steps: 1) the coating process, 2) the imprinting and the separating process, 3) any of the subsequent processes, which in this work is a film deposition over the imprinted nanostructures to make wire-grid polarizers. Material deposition is carried out in a separate machine.

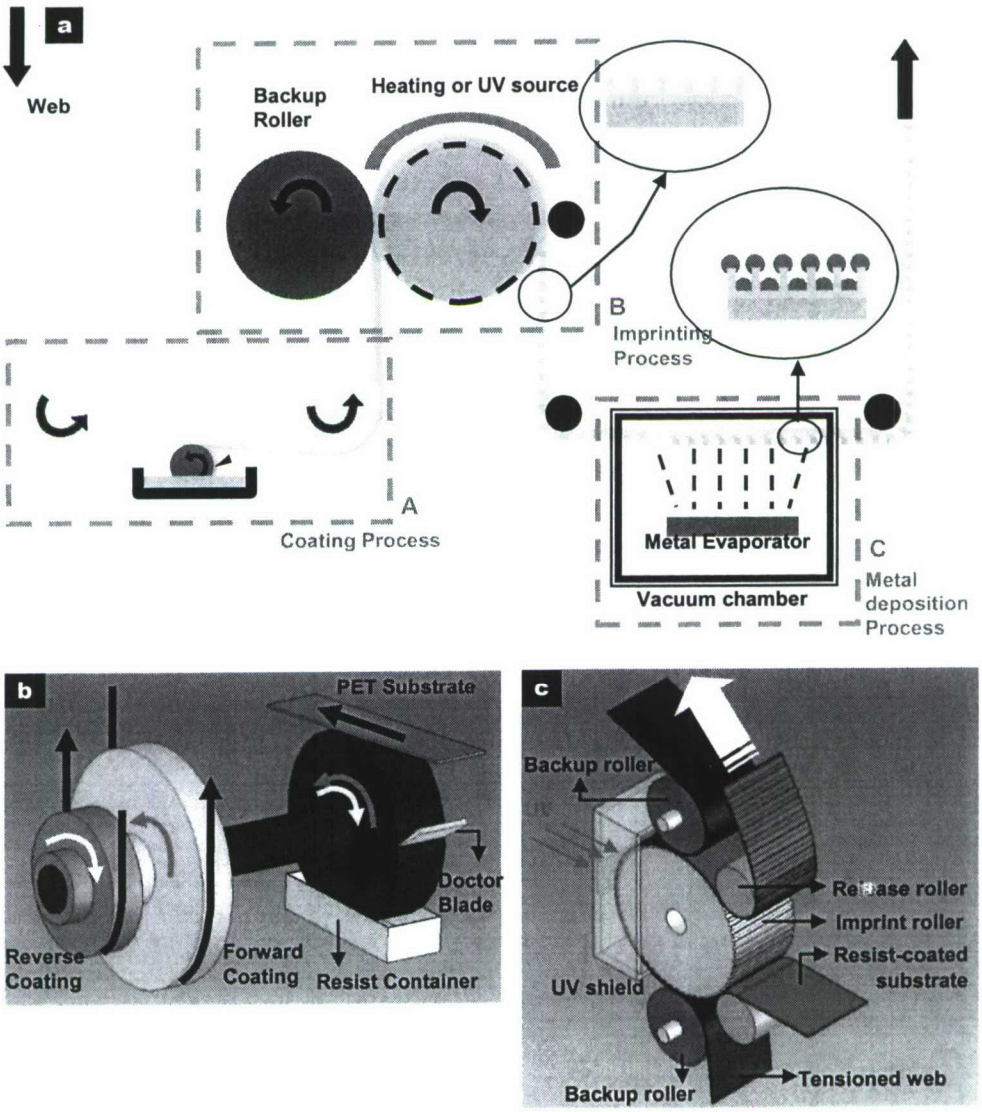

Figure 40. (a) Schematic of the R2RNIL process, and the continuous fabrication of metal wire-grid polarizer as one of its applications (the metal deposition is carried out in a separate evaporator in this study). (b) The coating unit and (c) the Imprint unit of the R2RNIL apparatus.

In the coating process, imprint resist is coated on the bare flexible substrate by reverse or forward coating system. Then, the liquid resist coated on the substrate is pressed with a flexible mold that is wrapped around a roller surface by both web tension and the pressure exerted by the backup rollers. Low-viscosity liquid resist [1,2] rapidly fills into the mold cavity. After that, resist is cured by heating or UV irradiation. We observe that faithful pattern is possible only if uniform pressure is applied during curing. Finally, mold

is released and the replicated nanostructures as the inverse pattern of mold remained on the flexible substrate.

(1) Coating Module

Resist thickness and its uniformity are very important for both pattern quality and from an economic point of view. Too thin a resist may cause defects due to insufficient filling into mold cavity or a low mechanical strength that results in film fracture during mold releasing. On the other hand, too thick a resist not only results in accumulation of resist after successive imprinting cycles and hampering further imprinting but also wastes resist material because excess resist can be squeezed out. We investigated two types of coating methods, reverse web coating and forward web coating (**Fig 40**). Reverse coating in which web direction is opposite to rolling direction provides uniform coating profile by eliminating film separation. However, coating tends to be thick and difficult to control due to stagnation of resist at the confluence point. On the other hand, forward coating provides thinner film layer but slightly lower surface uniformity than that of reverse coating. Another important feature of our R2RNIL coating module is the synchronized speed control of coating roller and the web speed. This guarantees uniform coating thickness regardless of web speed. Liquid resist from a container is transferred to a flexible PET substrate by coating roller and its thickness is controlled by a doctor blade.

(2) Imprinting module

Imprint section is the most important part in R2RNIL system because pattern quality is mostly determined by the pressure and curing conditions at the imprint roller. The Imprint module is composed of a imprint roller, backup rollers and a curing section. Flexible ethylene-tetrafluoroethylene (ETFE) mold is attached on the stainless steel imprint roller (diameter of 60 mm). Since the substrate is subjected to a normal force solely from the tensioned web, slip motion caused by tension of substrate can be minimized. Web tension can be adjusted by changing roll friction. Two backup rollers were used to guarantee non-slip rotation. Low-viscosity monomer resist quickly fills into mold cavity by web tension and the pressure from backup rollers. Without backup roller and tensioned web, slip may occur between the substrate and the mold surface due to non-uniform tension. Immediately after, the monomer resist is cured by heat or UV irradiation. For thermal curing, we used low-viscosity fast curable PDMS [1], which is cured by a heating gun; for UV cuing, we used UV curable epoxysilicone [2], which is exposed and cured by high-power UV source. We used a UV shield to confine the UV exposure only in the curing region, thus, it prevents premature curing of resist before filling into mold. Finally, PET substrate with the replicated nanostructures is separated from the from the mold on the roller by a release roller.

(3) Driving motor and speed controller

An AC motor with 180:1 gear head operates R2R system. Motor speed is controlled by speed controller (0.5 ~ 8.8 rpm) and rotating direction is switchable. A main driving pulley winds tensioned web and, also rotates coating roller connected to coating pulley.

Revolution speed of the imprint roller (diameter = 60 mm) is adjusted from 0.4 rpm to 7.5 rpm, thus, web speed varies from 1.3 mm/s to 23.5 mm/s. This driving system provides smooth motion with fine speed tuning, which is essential for high quality patterning.

5.2. R2RNIL results

period in our initial experiment, because well-replicated grating structure should show strong light diffraction and therefore the pattern quality can be easily examined by eye. A 200 mm long, 300 nm linewidth and 700 nm period gratings imprinted using the thermally cured PDMS on PET substrate are shown in Fig. 41a and 41b. Fig. 41c ~ 41e show UV R2RNIL results of a 570 mm long (width of 10 mm), 700 nm period grating structure created on PET substrate. Scanning electron microscopy (SEM) shows that the UV cured epoxysilicone resist pattern has higher quality than the thermal-cured PDMS, which can be attributed to the lower viscosity of the material that facilitates the fast filling of the mold cavity. Printing speed can be adjusted depending on the period of grating pattern and its aspect ratio. The fast curing of the resist material allow us to achieve a web speed of ~ 1 m/min.

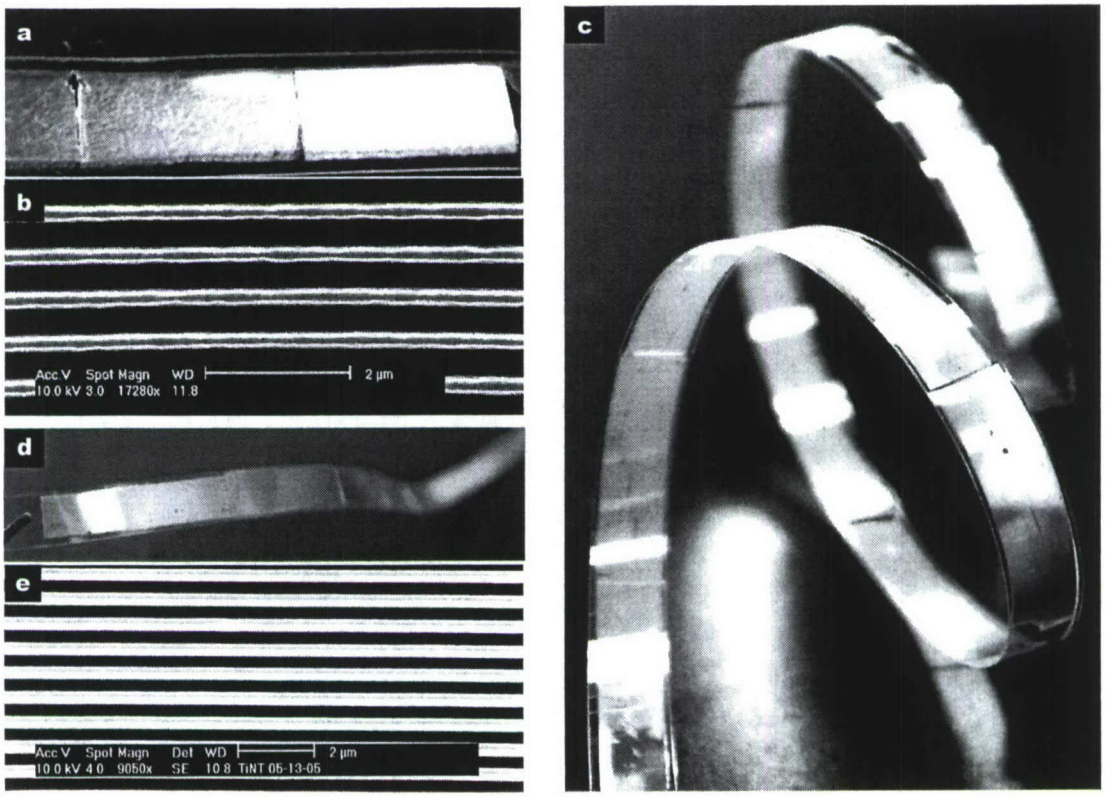

Figure 41. Thermal R2RNIL results: (a) Photograph of a 700 nm period, 300 nm line width PDMS grating pattern imprinted on PET strip by using the thermal R2RNIL and (b) the SEM micrograph of the replicated grating structure. UV R2RNIL results: (c), (d) Photographs of 700 nm period, 300 nm line width epoxysilicone grating pattern imprinted on PET strip by the UV R2RNIL, showing bright light diffraction and (e) the SEM of the replicated grating structure. Total length is 570 mm.

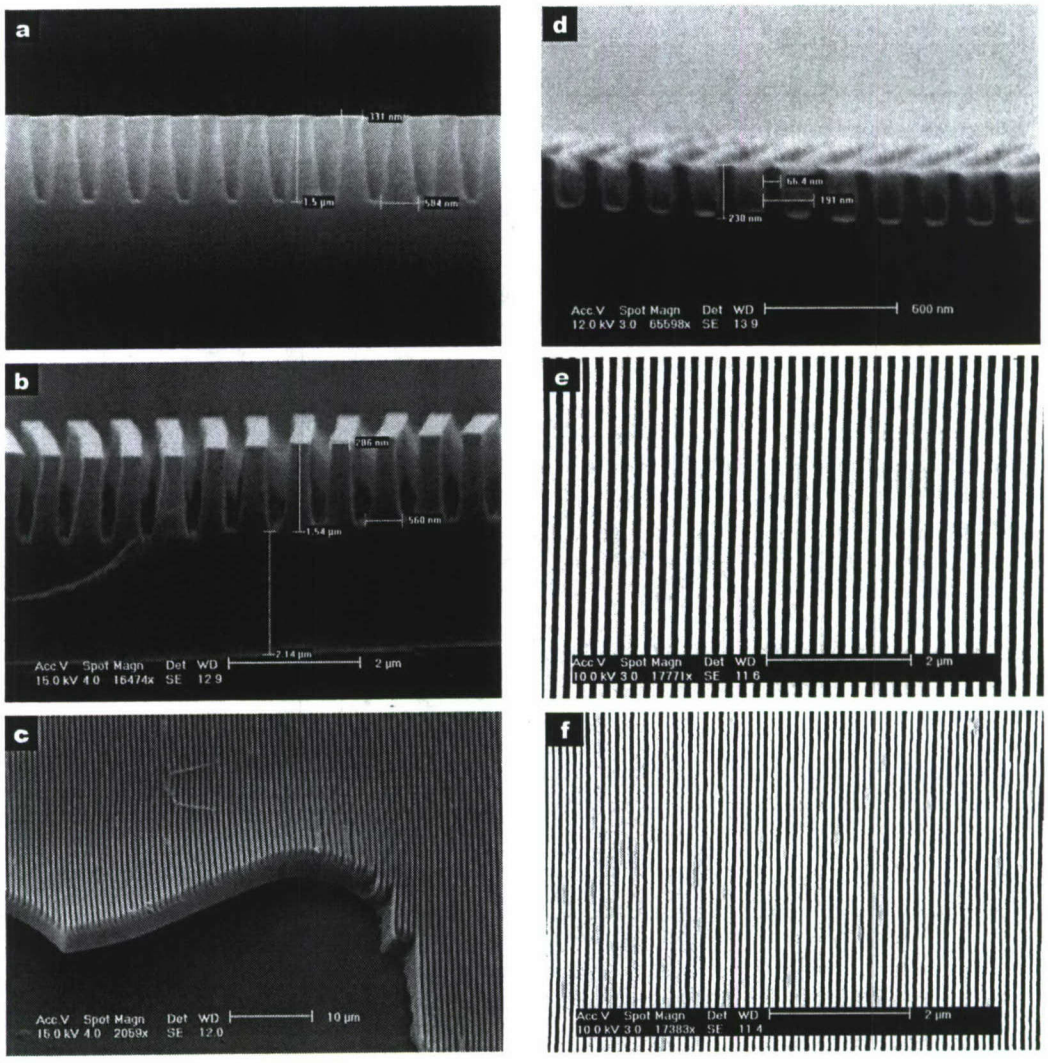

Figure 42. (a) The original Si mold. (b), (c) the epoxysilicone gratings replicated from the ETFE mold. (d), (e) SEM pictures of 200 nm period, 70 nm line width epoxysilicone pattern and (f) a 100 nm period, 70 nm line width epoxysilicone pattern fabricated by UV R2RNIL.

For easy visualization of the imprinting results, we chose a grating pattern of 700nm period in our initial experiment, because well-replicated grating structure should show strong light diffraction and therefore the pattern quality can be easily examined by eye. A 200 mm long, 300 nm linewidth and 700 nm period gratings imprinted using the thermally cured PDMS on PET substrate are shown in Fig. 41a and 41b. Fig. 41c ~ 41e show UV R2RNIL results of a 570 mm long (width of 10 mm), 700 nm period grating structure created on PET substrate. Scanning electron microscopy (SEM) shows that the UV cured epoxysilicone resist pattern has higher quality than the thermal-cured PDMS, which can be attributed to the lower viscosity of the material that facilitates the fast filling

of the mold cavity. Printing speed can be adjusted depending on the period of grating pattern and its aspect ratio. The fast curing of the resist material allow us to achieve a web speed of ~ 1 m/min.

High aspect ratio (AR = 5.4:1) grating structures with very sharp pattern definition fabricated by R2RNIL are shown in Fig. 42b and 42c. Faithfully replicated epoxysilicone pattern should have the same geometry as in the original Si mold (Fig. 42a) because the ETFE mold, replicated from the Si mold, has the exact inverse patterns of the Si mold. Comparing the grating structure on the original Si mold (Fig. 42a) and the imprinted epoxysilicone pattern (Fig. 42c), we observe excellent pattern replication even for the very fine details at the bottom of the grating trenches. Residual layer thickness in this result is about 2 ㎛, but can be controlled by web tension and backup roller pressure. Even though the ETFE mold has good anti-sticking property, such a high aspect ratio imprinted structure tends to show significant sticking to the ETFE mold due to the much larger contact area with the grating sidewalls on the mold. To achieve successful pattern transfer, oxygen plasma and surfactant treatment of PET surface was performed before imprinting, which improves the adhesion of the resist pattern to the PET substrate. Continuous roll-to-roll imprinting of thinner and denser grating structure is more challenging because such patterns are mechanically fragile, and tend to collapse during demolding if the trench is very small. This requires the cured resist to have sufficient modulus and yield strength. Good adhesion of the resist to the substrate is also very important for such denser structures, which was achieved by using the aforementioned adhesion promoter. Fig. 42d and 42e show 200 nm period, 70 nm linewidth epoxysilicone patterns by the UV R2RNIL process. SEM photograph of 100 nm period grating structure is also replicated successfully and shown in Fig. 42f.

5.3. Fabrication of metal wire-grid polarizer by R2R process

To demonstrate an application of the R2RNIL process, we fabricated a metal wire-grid polarizer [4]. By depositing a thin metal (Al) layer over the imprinted grating structures (Fig. 43), high-efficiency polarizer in the form of bilayer metal wire grating can be achieved [5]. In our initial experiment, a 200 nm and 100 nm period grating pattern (Fig. 42d ~ 42f) were prepared by the R2RNIL process and various thickness of aluminum was thermally deposited on top of the grating as well as at the bottom of the trench (Fig. 44a). The bilayer metal wire-grid can be considered as two metal gratings separated by a certain distance. Not only this type of new polarizer provides very high extinction ratio between lights of two orthogonal polarizations, but it offers the great advantage easy fabrication and defect tolerance. As the final step is evaporation of the metal film, the fabrication process is self-masking, which means that defects on the nanostructured areas and unstructured areas that may exist on the substrate are automatically covered by an opaque metal film. Thus, the fabrication is robust against pinhole generation whereas in fabrication methods that incorporate metal etching or lift-off steps, defects can lead to pinholes. Such defects constitute one of the major limitations on the polarizing performance in particular when high extinction ratios are aimed.

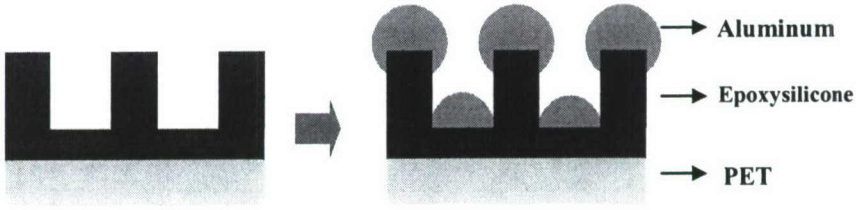

Fig.43 Schematics of fabrication process of metal wire-grid polarizer

To quantify the polarization effect, spectral transmittance was measured using UV/Vis spectrometer. Fig. 44b shows the transmittance of the TM, TE polarized light through the fabricated metal wire-grid polarizer. The best polarizer result was obtained from the 100 nm period grating with 50 nm Al layer, with transmittance ~ 30 % at 800 nm wavelength and extinction ratio (transmittance of TM / transmittance of TE) over 2,000 at 700 ~ 800 nm wavelength. We would like to point out that in these preliminary experiments, many parameters such as grating period, line width and metal thickness have not yet been optimized.

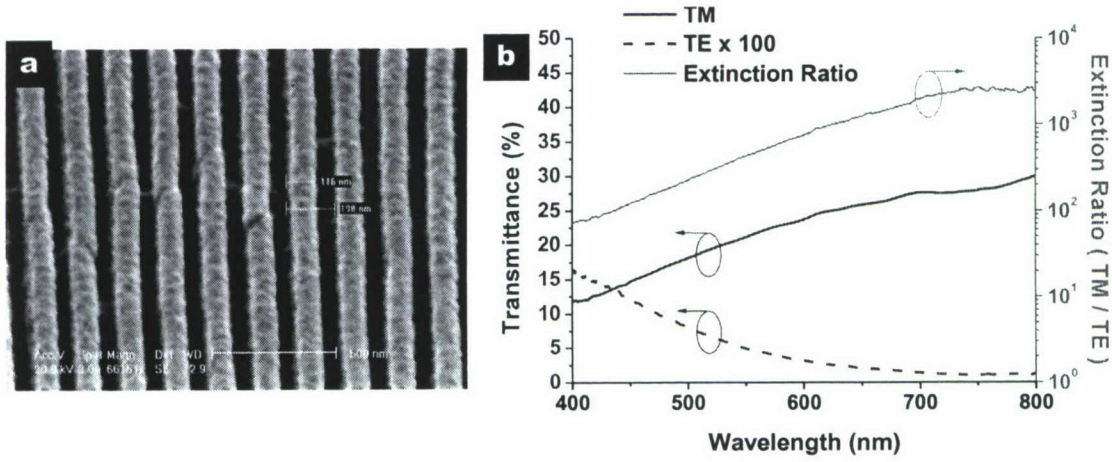

Figure 44. (a) SEM picture of a 200 nm period grating with 50 nm Al on top. (b) Spectral transmittance (TM, TE mode) and extinction ratio (TM/TE) of metal wire-grid polarizer fabricated by R2RNIL.

References:

[1] C. P.-Hernandez, J.-S. Kim, L. J. Guo, and P.-F. Fu, "High throughput and etch selective nanoimprinting and stamping based on fast thermal-curable polydimethysiloxanes," *Adv. Mater.* 2007, in press.

[2] X. Cheng, L. J. Guo, and P.-F. Fu, "Room Temperature and Low Pressure Nanoimprinting Based on Cationic Photopolymerization of Novel Epoxysilicone Monomers," *Adv. Mat.*, Vol. 17, pp. 1419-1424, 2005.

[3] S. H. Ahn, and L. J. Guo, "High Speed Roll-to-Roll Nanoimprint Lithography on Flexible Plastic Substrate," *Adv. Mater*, 2008, in press.

[4] S. H. Ahn, J. Kim and L. J. Guo, "Bilayer Metal Wire-grid Polarizer Fabricated by Roll-to-Roll Nanoimprint Lithography on Flexible Plastic Substrate," *J. Vac. Sci. & Technol.* B. 25(6), 2388-2391, 2007.

[5] Y. Ekinci, H. Solak, C. David and H. Sigg, "Bilayer Al wire-grids as broadband and highperformance polarizers," *Optics Express*, Vol. 14, No. 6, 2006.